

FEATURES

- Low offset voltage:** 5 μV maximum
- Extremely low offset drift:** 22 $\text{nV}/^\circ\text{C}$ maximum
- Low voltage noise:** 5.8 $\text{nV}/\sqrt{\text{Hz}}$ typical
117 nV p-p from 0.1 Hz to 10 Hz typical
- Low input bias current:** 50 pA typical
- Unity-gain crossover:** 3 MHz
- Single-supply operation:** input voltage range includes ground and rail-to-rail output
- Wide range of operating voltages**
 - Single-supply operation: 4.5 V to 55 V
 - Dual-supply operation: ± 2.25 V to ± 27.5 V
- Integrated EMI filters**
- Unity-gain stable**

APPLICATIONS

- LCR meter/megohmmeter front-end amplifiers
- Load cell and bridge transducers
- Magnetic force balance scales
- High precision shunt current sensing
- Thermocouple/RTD sensors
- PLC input and output amplifiers

GENERAL DESCRIPTION

The ADA4522-2 is a dual channel, zero drift op amp with low noise and power, ground sensing inputs, and rail-to-rail output, optimized for total accuracy over time, temperature, and voltage conditions. The wide operating voltage and temperature ranges, as well as the high open-loop gain and very low dc and ac errors make the device well suited for amplifying very small input signals and for accurately reproducing larger signals in a wide variety of applications.

The ADA4522-2 performance is specified at 5.0 V, 30 V, and 55 V power supply voltages and it operates over the range of 4.5 V to 55 V. It is an excellent selection for applications using single-ended supplies of 5 V, 10 V, 12 V, and 30 V, or for applications using higher single supplies and dual supplies of ± 2.5 V, ± 5 V, and ± 15 V. The ADA4522-2 uses on-chip filtering to achieve high immunity to electromagnetic interference (EMI).

The ADA4522-2 is fully specified over the extended industrial temperature range of -40°C to $+125^\circ\text{C}$ and is available in 8-lead MSOP and 8-lead SOIC packages.

PIN CONNECTION DIAGRAM



Figure 1. 8-Lead MSOP (RM Suffix) and 8-Lead SOIC (R Suffix) Pin Configuration



Figure 2. Voltage Noise Density, $V_{SY} = \pm 15\text{V}$

Table 1. Zero Drift Op Amps ($<0.1 \mu\text{V}/^\circ\text{C}$)

Supply Voltage	5 V	16 V	30 V	55 V
Single	ADA4528-1 AD8628 AD8538 ADA4051-1	AD8638	ADA4638-1	
Dual	ADA4528-2 AD8629 AD8539 ADA4051-2	AD8639		ADA4522-2
Quad	AD8630			

Rev. 0

[Document Feedback](#)

Information furnished by Analog Devices is believed to be accurate and reliable. However, no responsibility is assumed by Analog Devices for its use, nor for any infringements of patents or other rights of third parties that may result from its use. Specifications subject to change without notice. No license is granted by implication or otherwise under any patent or patent rights of Analog Devices. Trademarks and registered trademarks are the property of their respective owners.

TABLE OF CONTENTS

Features	1	On-Chip Input EMI Filter and Clamp Circuit.....	20
Applications.....	1	Thermal Shutdown	21
Pin Connection Diagram	1	Input Protection	21
General Description	1	Single Supply and Rail-to-Rail Output.....	21
Revision History	2	Large Signal Transient Response.....	22
Specifications.....	3	Noise Considerations.....	22
Electrical Characteristics—5.0 V Operation	3	EMI Rejection Ratio	24
Electrical Characteristics—30 V Operation	4	Single-Supply Instrumentation Amplifier	24
Electrical Characteristics—55 V Operation	5	Load Cell/Strain Gage Sensor Signal Conditioning	25
Absolute Maximum Ratings.....	7	Precision Low-Side Current Shunt Sensor.....	26
Thermal Resistance	7	Printed Circuit Board Layout	26
ESD Caution.....	7	Comparator Operation.....	27
Pin Configuration and Function Descriptions.....	8	Outline Dimensions	28
Typical Performance Characteristics	9	Ordering Guide	28
Applications Information	20		
Theory of Operation	20		

REVISION HISTORY

5/15—Revision 0: Initial Version

SPECIFICATIONS

ELECTRICAL CHARACTERISTICS—5.0 V OPERATION

$V_{SY} = 5.0\text{ V}$, $V_{CM} = V_{SY}/2$, $T_A = 25^\circ\text{C}$, unless otherwise specified.

Table 2.

Parameter	Symbol	Test Conditions/Comments	Min	Typ	Max	Unit
INPUT CHARACTERISTICS						
Offset Voltage	V_{OS}	$V_{CM} = V_{SY}/2$ $-40^\circ\text{C} \leq T_A \leq +125^\circ\text{C}$		0.7	5	μV
Offset Voltage Drift	$\Delta V_{OS}/\Delta T$			2.5	15	$\text{nV}/^\circ\text{C}$
Input Bias Current	I_B	$-40^\circ\text{C} \leq T_A \leq +85^\circ\text{C}$ $-40^\circ\text{C} \leq T_A \leq +125^\circ\text{C}$		50	150	pA
Input Offset Current	I_{OS}	$-40^\circ\text{C} \leq T_A \leq +85^\circ\text{C}$ $-40^\circ\text{C} \leq T_A \leq +125^\circ\text{C}$		80	250	pA
Input Voltage Range	IVR		0		3.5	V
Common-Mode Rejection Ratio	CMRR	$V_{CM} = 0\text{ V to } 3.5\text{ V}$ $-40^\circ\text{C} \leq T_A \leq +125^\circ\text{C}$	135	155		dB
Large Signal Voltage Gain	A_{VO}	$R_L = 10\text{ k}\Omega$, $V_{OUT} = 0.5\text{ V to } 4.5\text{ V}$ $-40^\circ\text{C} \leq T_A \leq +125^\circ\text{C}$	125	145		dB
Input Resistance						
Differential Mode	R_{INDM}			30		$\text{k}\Omega$
Common Mode	R_{INCM}			100		$\text{G}\Omega$
Input Capacitance						
Differential Mode	C_{INDM}			7		pF
Common Mode	C_{INCM}			35		pF
OUTPUT CHARACTERISTICS						
Output Voltage High	V_{OH}	$R_L = 10\text{ k}\Omega$ to $V_{SY}/2$ $-40^\circ\text{C} \leq T_A \leq +125^\circ\text{C}$	4.97	4.98		V
Output Voltage Low	V_{OL}	$R_L = 10\text{ k}\Omega$ to $V_{SY}/2$ $-40^\circ\text{C} \leq T_A \leq +125^\circ\text{C}$	4.95	20	30	mV
Continuous Output Current	I_{OUT}	Dropout voltage = 1 V		14		mA
Short-Circuit Current Source	I_{SC+}	$T_A = 125^\circ\text{C}$		22		mA
Short-Circuit Current Sink	I_{SC-}	$T_A = 125^\circ\text{C}$		15		mA
Closed-Loop Output Impedance	Z_{OUT}	$f = 1\text{ MHz}$, $A_v = +1$		29		mA
POWER SUPPLY						
Power Supply Rejection Ratio	PSRR	$V_{SY} = 4.5\text{ V to } 55\text{ V}$ $-40^\circ\text{C} \leq T_A \leq +125^\circ\text{C}$	150	160		dB
Supply Current per Amplifier	I_{SY}	$I_{OUT} = 0\text{ mA}$ $-40^\circ\text{C} \leq T_A \leq +125^\circ\text{C}$	145	830	900	μA
DYNAMIC PERFORMANCE						
Slew Rate	SR+	$R_L = 10\text{ k}\Omega$, $C_L = 50\text{ pF}$, $A_v = 1$		1.4		$\text{V}/\mu\text{s}$
	SR-	$R_L = 10\text{ k}\Omega$, $C_L = 50\text{ pF}$, $A_v = 1$		1.3		$\text{V}/\mu\text{s}$
Gain Bandwidth Product	GBP	$V_{IN} = 10\text{ mV p-p}$, $R_L = 10\text{ k}\Omega$, $C_L = 50\text{ pF}$, $A_{VO} = 100$		2.7		MHz
Unity-Gain Crossover	UGC	$V_{IN} = 10\text{ mV p-p}$, $R_L = 10\text{ k}\Omega$, $C_L = 50\text{ pF}$, $A_{VO} = 1$		3		MHz
-3 dB Closed-Loop Bandwidth	f_{-3dB}	$V_{IN} = 10\text{ mV p-p}$, $R_L = 10\text{ k}\Omega$, $C_L = 50\text{ pF}$, $A_v = 1$		6.5		MHz
Phase Margin	ΦM	$V_{IN} = 10\text{ mV p-p}$, $R_L = 10\text{ k}\Omega$, $C_L = 50\text{ pF}$, $A_{VO} = 1$		64		Degrees
Settling Time to 0.1%	t_s	$V_{IN} = 1\text{ V step}$, $R_L = 10\text{ k}\Omega$, $C_L = 50\text{ pF}$, $A_v = 1$		4		μs
Channel Separation	CS	$V_{IN} = 1\text{ V p-p}$, $f = 10\text{ kHz}$, $R_L = 10\text{ k}\Omega$, $C_L = 50\text{ pF}$		98		dB

Parameter	Symbol	Test Conditions/Comments	Min	Typ	Max	Unit
EMI Rejection Ratio of +IN x	EMIRR	$V_{IN} = 100 \text{ mV}_{PEAK}, f = 400 \text{ MHz}$		72		dB
		$V_{IN} = 100 \text{ mV}_{PEAK}, f = 900 \text{ MHz}$		80		dB
		$V_{IN} = 100 \text{ mV}_{PEAK}, f = 1800 \text{ MHz}$		83		dB
		$V_{IN} = 100 \text{ mV}_{PEAK}, f = 2400 \text{ MHz}$		85		dB
NOISE PERFORMANCE						
Total Harmonic Distortion + Noise Bandwidth (BW) = 80 kHz BW = 500 kHz	THD + N	$A_V = +1, f = 1 \text{ kHz}, V_{IN} = 0.6 \text{ V rms}$		0.001		%
				0.02		%
Peak-to-Peak Voltage Noise	$e_{N \text{ p-p}}$	$A_V = 100, f = 0.1 \text{ Hz to } 10 \text{ Hz}$		117		nV p-p
Voltage Noise Density	e_N	$A_V = 100, f = 1 \text{ kHz}$		5.8		nV/ $\sqrt{\text{Hz}}$
Peak-to-Peak Current Noise	$i_{N \text{ p-p}}$	$A_V = 100, f = 0.1 \text{ Hz to } 10 \text{ Hz}$		16		pA p-p
Current Noise Density	i_N	$A_V = 100, f = 1 \text{ kHz}$		0.8		pA/ $\sqrt{\text{Hz}}$

ELECTRICAL CHARACTERISTICS—30 V OPERATION

$V_{SY} = 30 \text{ V}, V_{CM} = V_{SY}/2 \text{ V}, T_A = 25^\circ\text{C}$, unless otherwise specified.

Table 3.

Parameter	Symbol	Test Conditions/Comments	Min	Typ	Max	Unit
INPUT CHARACTERISTICS						
Offset Voltage	V_{OS}	$V_{CM} = V_{SY}/2$ $-40^\circ\text{C} \leq T_A \leq +125^\circ\text{C}$		1	5	μV
Offset Voltage Drift	$\Delta V_{OS}/\Delta T$			4	22	nV/ $^\circ\text{C}$
Input Bias Current	I_B	$-40^\circ\text{C} \leq T_A \leq +85^\circ\text{C}$		50	150	pA
		$-40^\circ\text{C} \leq T_A \leq +125^\circ\text{C}$			500	pA
Input Offset Current	I_{OS}	$-40^\circ\text{C} \leq T_A \leq +85^\circ\text{C}$			3	nA
		$-40^\circ\text{C} \leq T_A \leq +125^\circ\text{C}$		80	300	pA
						400
Input Voltage Range	IVR	$-40^\circ\text{C} \leq T_A \leq +125^\circ\text{C}$	0		28.5	V
Common-Mode Rejection Ratio	CMRR	$V_{CM} = 0 \text{ V to } 28.5 \text{ V}$ $-40^\circ\text{C} \leq T_A \leq +125^\circ\text{C}$	145	160		dB
			140			dB
Large Signal Voltage Gain	A_{VO}	$R_L = 10 \text{ k}\Omega, V_{OUT} = 0.5 \text{ V to } 29.5 \text{ V}$ $-40^\circ\text{C} \leq T_A \leq +125^\circ\text{C}$	140	150		dB
			135			dB
Input Resistance	R_{INDM} R_{INCM}			30		k Ω
				400		G Ω
Input Capacitance	C_{INDM} C_{INCM}			7		pF
				35		pF
OUTPUT CHARACTERISTICS						
Output Voltage High	V_{OH}	$R_L = 10 \text{ k}\Omega \text{ to } V_{SY}/2$ $-40^\circ\text{C} \leq T_A \leq +125^\circ\text{C}$	29.87	29.89		V
			29.80			V
Output Voltage Low	V_{OL}	$R_L = 10 \text{ k}\Omega \text{ to } V_{SY}/2$ $-40^\circ\text{C} \leq T_A \leq +125^\circ\text{C}$		110	130	mV
					200	mV
Continuous Output Current	I_{OUT}	Dropout voltage = 1 V		14		mA
Short-Circuit Current Source	I_{SC+}	$T_A = +125^\circ\text{C}$		21		mA
				15		mA
Short-Circuit Current Sink	I_{SC-}	$T_A = +125^\circ\text{C}$		33		mA
				22		mA
Closed-Loop Output Impedance	Z_{OUT}	$f = 1 \text{ MHz}, A_V = +1$		4		Ω

Parameter	Symbol	Test Conditions/Comments	Min	Typ	Max	Unit
POWER SUPPLY						
Power Supply Rejection Ratio	PSRR	$V_{SY} = 4.5\text{ V to }55\text{ V}$ $-40^{\circ}\text{C} \leq T_A \leq +125^{\circ}\text{C}$	150	160		dB
Supply Current per Amplifier	I_{SY}	$I_{OUT} = 0\text{ mA}$ $-40^{\circ}\text{C} \leq T_A \leq +125^{\circ}\text{C}$	145	830	900	dB μA μA
DYNAMIC PERFORMANCE						
Slew Rate	SR+	$R_L = 10\text{ k}\Omega$, $C_L = 50\text{ pF}$, $A_V = 1$		1.8		V/ μs
	SR-	$R_L = 10\text{ k}\Omega$, $C_L = 50\text{ pF}$, $A_V = 1$		0.9		V/ μs
Gain Bandwidth Product	GBP	$V_{IN} = 10\text{ mV p-p}$, $R_L = 10\text{ k}\Omega$, $C_L = 50\text{ pF}$, $A_{VO} = 100$		2.7		MHz
Unity-Gain Crossover	UGC	$V_{IN} = 10\text{ mV p-p}$, $R_L = 10\text{ k}\Omega$, $C_L = 50\text{ pF}$, $A_{VO} = 1$		3		MHz
-3 dB Closed-Loop Bandwidth	$f_{-3\text{ dB}}$	$V_{IN} = 10\text{ mV p-p}$, $R_L = 10\text{ k}\Omega$, $C_L = 50\text{ pF}$, $A_V = 1$		6.5		MHz
Phase Margin	Φ_M	$V_{IN} = 10\text{ mV p-p}$, $R_L = 10\text{ k}\Omega$, $C_L = 50\text{ pF}$, $A_{VO} = 1$		64		Degrees
Settling Time to 0.1%	t_S	$V_{IN} = 10\text{ V step}$, $R_L = 10\text{ k}\Omega$, $C_L = 50\text{ pF}$, $A_V = 1$		12		μs
Settling Time to 0.01%	t_S	$V_{IN} = 10\text{ V step}$, $R_L = 10\text{ k}\Omega$, $C_L = 50\text{ pF}$, $A_V = 1$		14		μs
Channel Separation	CS	$V_{IN} = 10\text{ V p-p}$, $f = 10\text{ kHz}$, $R_L = 10\text{ k}\Omega$, $C_L = 50\text{ pF}$		98		dB
EMI Rejection Ratio of +IN x	EMIRR	$V_{IN} = 100\text{ mV}_{PEAK}$, $f = 400\text{ MHz}$		72		dB
		$V_{IN} = 100\text{ mV}_{PEAK}$, $f = 900\text{ MHz}$		80		dB
		$V_{IN} = 100\text{ mV}_{PEAK}$, $f = 1800\text{ MHz}$		83		dB
		$V_{IN} = 100\text{ mV}_{PEAK}$, $f = 2400\text{ MHz}$		85		dB
NOISE PERFORMANCE						
Total Harmonic Distortion + Noise	THD + N	$A_V = +1$, $f = 1\text{ kHz}$, $V_{IN} = 6\text{ V rms}$		0.0005		%
BW = 80 kHz				0.004		%
BW = 500 kHz						
Peak-to-Peak Voltage Noise	$e_{N\text{ p-p}}$	$A_V = 100$, $f = 0.1\text{ Hz to }10\text{ Hz}$		117		nV p-p
Voltage Noise Density	e_N	$A_V = 100$, $f = 1\text{ kHz}$		5.8		nV/ $\sqrt{\text{Hz}}$
Peak-to-Peak Current Noise	$i_{N\text{ p-p}}$	$A_V = 100$, $f = 0.1\text{ Hz to }10\text{ Hz}$		16		pA p-p
Current Noise Density	i_N	$A_V = 100$, $f = 1\text{ kHz}$		0.8		pA/ $\sqrt{\text{Hz}}$

ELECTRICAL CHARACTERISTICS—55 V OPERATION

$V_{SY} = 55\text{ V}$, $V_{CM} = V_{SY}/2\text{ V}$, $T_A = 25^{\circ}\text{C}$, unless otherwise specified.

Table 4.

Parameter	Symbol	Test Conditions/Comments	Min	Typ	Max	Unit
INPUT CHARACTERISTICS						
Offset Voltage	V_{OS}	$V_{CM} = V_{SY}/2$ $-40^{\circ}\text{C} \leq T_A \leq +125^{\circ}\text{C}$		1.5	7	μV
Offset Voltage Drift	$\Delta V_{OS}/\Delta T$			6	30	nV/ $^{\circ}\text{C}$
Input Bias Current	I_B	$-40^{\circ}\text{C} \leq T_A \leq +85^{\circ}\text{C}$ $-40^{\circ}\text{C} \leq T_A \leq +125^{\circ}\text{C}$		50	150	pA
Input Offset Current	I_{OS}	$-40^{\circ}\text{C} \leq T_A \leq +85^{\circ}\text{C}$ $-40^{\circ}\text{C} \leq T_A \leq +125^{\circ}\text{C}$		80	300	pA
Input Voltage Range	IVR		0		53.5	V
Common-Mode Rejection Ratio	CMRR	$V_{CM} = 0\text{ V to }53.5\text{ V}$ $-40^{\circ}\text{C} \leq T_A \leq +125^{\circ}\text{C}$	140	144		dB
Large Signal Voltage Gain	A_{VO}	$R_L = 10\text{ k}\Omega$, $V_{OUT} = 0.5\text{ V to }54.5\text{ V}$ $-40^{\circ}\text{C} \leq T_A \leq +125^{\circ}\text{C}$	135	137		dB
Input Resistance			125			dB
Differential Mode	R_{INDM}			30		k Ω
Common Mode	R_{INCM}			1000		G Ω

Parameter	Symbol	Test Conditions/Comments	Min	Typ	Max	Unit
Input Capacitance						
Differential Mode	C _{INDM}			7		pF
Common Mode	C _{INCM}			35		pF
OUTPUT CHARACTERISTICS						
Output Voltage High	V _{OH}	R _L = 10 kΩ to V _{SY} /2 −40°C ≤ T _A ≤ +125°C	54.75 54.65	54.8		V V
Output Voltage Low	V _{OL}	R _L = 10 kΩ to V _{SY} /2 −40°C ≤ T _A ≤ +125°C		200	250 350	mV mV
Continuous Output Current	I _{OUT}	Dropout voltage = 1 V		14		mA
Short-Circuit Current Source	I _{SC+}	T _A = 125°C		21		mA
Short-Circuit Current Sink	I _{SC−}	T _A = 125°C		15		mA
Closed-Loop Output Impedance	Z _{OUT}	T _A = 125°C f = 1 MHz, A _v = +1		32		mA
				22		Ω
				4		
POWER SUPPLY						
Power Supply Rejection Ratio	PSRR	V _{SY} = 4.5 V to 55 V −40°C ≤ T _A ≤ +125°C	150 145	160		dB dB
Supply Current per Amplifier	I _{SY}	I _{OUT} = 0 mA −40°C ≤ T _A ≤ +125°C		830	900 950	μA μA
DYNAMIC PERFORMANCE						
Slew Rate	SR+	R _L = 10 kΩ, C _L = 50 pF, A _v = 1		1.7		V/μs
	SR−	R _L = 10 kΩ, C _L = 50 pF, A _v = 1		0.8		V/μs
Gain Bandwidth Product	GBP	V _{IN} = 10 mV p-p, R _L = 10 kΩ, C _L = 50 pF, A _{VO} = 100		2.7		MHz
Unity-Gain Crossover	UGC	V _{IN} = 10 mV p-p, R _L = 10 kΩ, C _L = 50 pF, A _{VO} = 1		3		MHz
−3 dB Closed-Loop Bandwidth	f _{−3 dB}	V _{IN} = 10 mV p-p, R _L = 10 kΩ, C _L = 50 pF, A _v = 1		6.5		MHz
Phase Margin	Φ _M	V _{IN} = 10 mV p-p, R _L = 10 kΩ, C _L = 50 pF, A _{VO} = 1		64		Degrees
Settling Time to 0.1%	t _s	V _{IN} = 10 V step, R _L = 10 kΩ, C _L = 50 pF, A _v = 1		12		μs
Settling Time to 0.01%	t _s	V _{IN} = 10 V step, R _L = 10 kΩ, C _L = 50 pF, A _v = 1		14		μs
Channel Separation	CS	V _{IN} = 10 V p-p, f = 10 kHz, R _L = 10 kΩ, C _L = 50 pF		98		dB
EMI Rejection Ratio of +IN x	EMIRR	V _{IN} = 100 mV _{PEAK} , f = 400 MHz		72		dB
		V _{IN} = 100 mV _{PEAK} , f = 900 MHz		80		dB
		V _{IN} = 100 mV _{PEAK} , f = 1800 MHz		83		dB
		V _{IN} = 100 mV _{PEAK} , f = 2400 MHz		85		dB
NOISE PERFORMANCE						
Total Harmonic Distortion + Noise	THD + N	A _v = +1, f = 1 kHz, V _{IN} = 10 V rms		0.0007		%
BW = 80 kHz				0.003		%
BW = 500 kHz						
Peak-to-Peak Voltage Noise	e _{N p-p}	A _v = 100, f = 0.1 Hz to 10 Hz		117		nV p-p
Voltage Noise Density	e _N	A _v = 100, f = 1 kHz		5.8		nV/√Hz
Peak-to-Peak Current Noise	i _{N p-p}	A _v = 100, f = 0.1 Hz to 10 Hz		16		pA p-p
Current Noise Density	i _N	A _v = 100, f = 1 kHz		0.8		pA/√Hz

ABSOLUTE MAXIMUM RATINGS

Table 5.

Parameter	Rating
Supply Voltage	60 V
Input Voltage	(V ₋) – 300 mV to (V ₊) + 300 mV
Input Current ¹	±10 mA
Differential Input Voltage	±5 V
Output Short-Circuit Duration to Ground	Indefinite
Temperature Range	
Storage	–65°C to +150°C
Operating	–40°C to +125°C
Junction	–65°C to +150°C
Lead Temperature (Soldering, 60 sec)	300°C

¹ The input pins have clamp diodes to the power supply pins. Limit the input current to 10 mA or less whenever input signals exceed the power supply rail by 0.3 V.

Stresses at or above those listed under Absolute Maximum Ratings may cause permanent damage to the product. This is a stress rating only; functional operation of the product at these or any other conditions above those indicated in the operational section of this specification is not implied. Operation beyond the maximum operating conditions for extended periods may affect product reliability.

THERMAL RESISTANCE

θ_{JA} is specified for the worst case conditions, that is, a device soldered in a circuit board for surface-mount packages using a standard 4-layer JEDEC board.

Table 6. Thermal Resistance

Package Type	θ_{JA}	θ_{JC}	Unit
8-Lead MSOP (RM-8)	190	44	°C/W
8-Lead SOIC (R-8)	158	43	°C/W

ESD CAUTION



ESD (electrostatic discharge) sensitive device. Charged devices and circuit boards can discharge without detection. Although this product features patented or proprietary protection circuitry, damage may occur on devices subjected to high energy ESD. Therefore, proper ESD precautions should be taken to avoid performance degradation or loss of functionality.

PIN CONFIGURATION AND FUNCTION DESCRIPTIONS



Figure 3. Pin Configuration

Table 7. Pin Function Descriptions

Pin No.	Mnemonic	Description
1	OUT A	Output, Channel A
2	-IN A	Inverting Input, Channel A
3	+IN A	Noninverting Input, Channel A
4	V-	Negative Supply Voltage
5	+IN B	Noninverting Input, Channel B
6	-IN B	Inverting Input, Channel B
7	OUT B	Output, Channel B
8	V+	Positive Supply Voltage

TYPICAL PERFORMANCE CHARACTERISTICS

T_A = 25°C, unless otherwise noted.

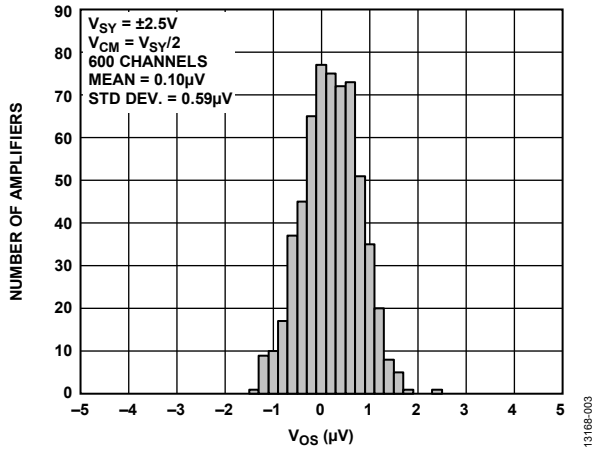


Figure 4. Input Offset Voltage Distribution, V_{SY} = ±2.5 V

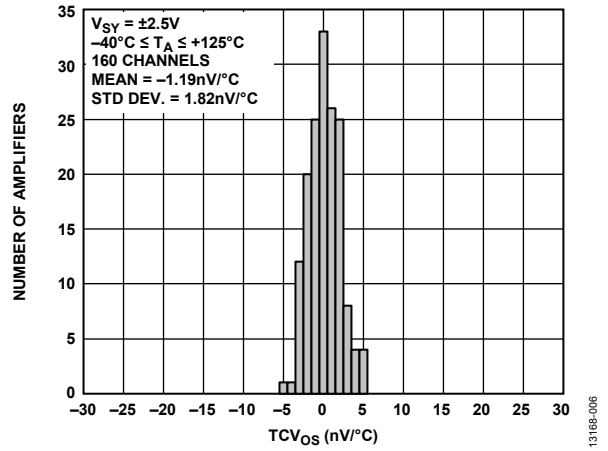


Figure 7. Input Offset Voltage Drift Distribution, V_{SY} = ±2.5 V

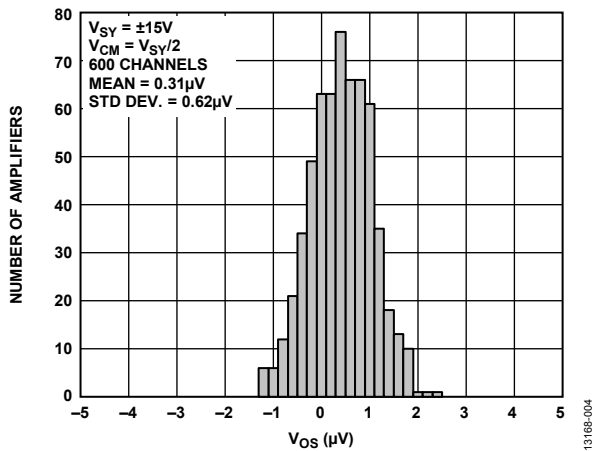


Figure 5. Input Offset Voltage Distribution, V_{SY} = ±15 V

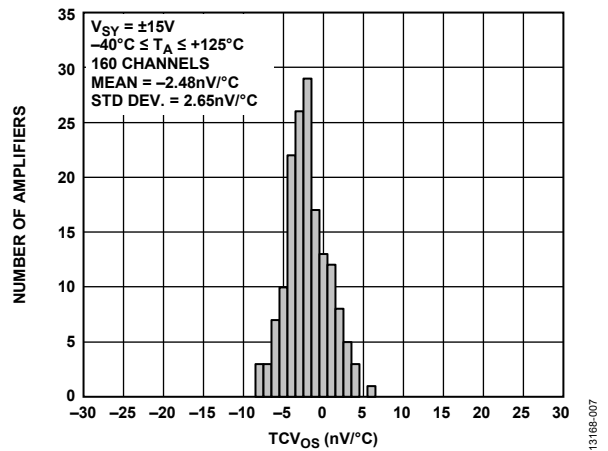


Figure 8. Input Offset Voltage Drift Distribution, V_{SY} = ±15 V



Figure 6. Input Offset Voltage Distribution, V_{SY} = ±27.5 V



Figure 9. Input Offset Voltage Drift Distribution, V_{SY} = ±27.5 V



Figure 10. Input Offset Voltage (V_{OS}) vs. Common-Mode Voltage (V_{CM}), $V_{SY} = 5V$

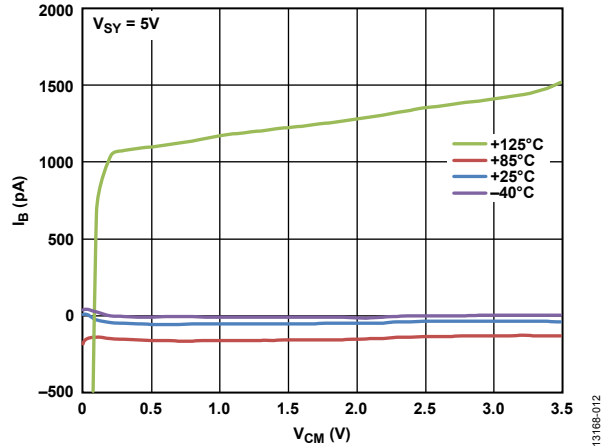


Figure 13. Input Bias Current (I_B) vs. Common-Mode Voltage (V_{CM}), $V_{SY} = 5V$



Figure 11. Input Offset Voltage (V_{OS}) vs. Common-Mode Voltage (V_{CM}), $V_{SY} = 30V$

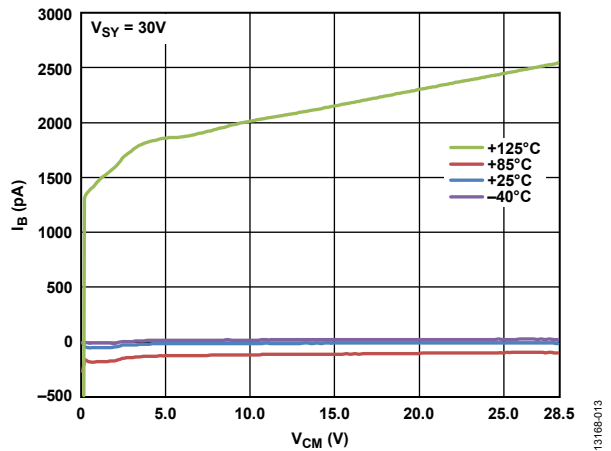


Figure 14. Input Bias Current (I_B) vs. Common-Mode Voltage (V_{CM}), $V_{SY} = 30V$

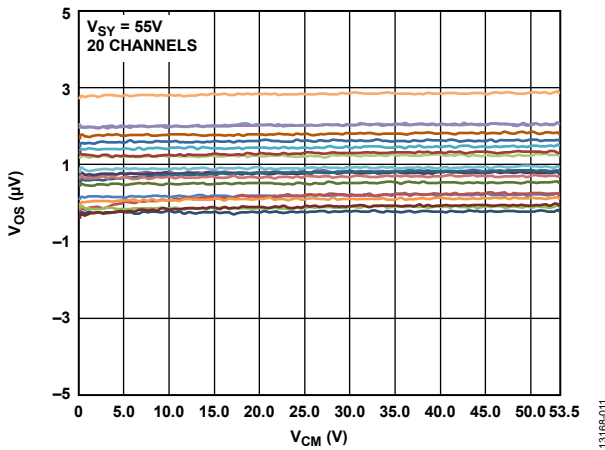


Figure 12. Input Offset Voltage (V_{OS}) vs. Common-Mode Voltage (V_{CM}), $V_{SY} = 55V$

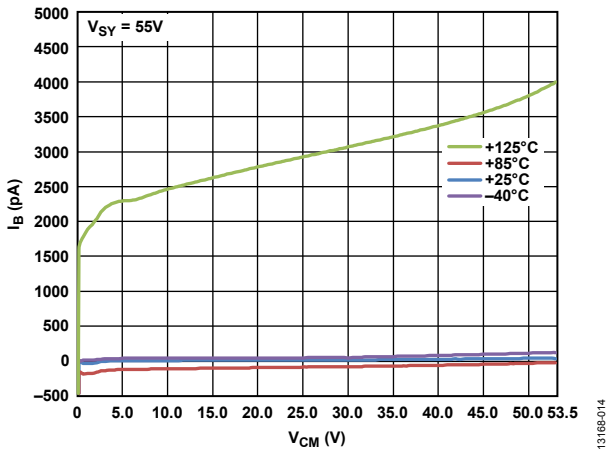


Figure 15. Input Bias Current (I_B) vs. Common-Mode Voltage (V_{CM}), $V_{SY} = 55V$

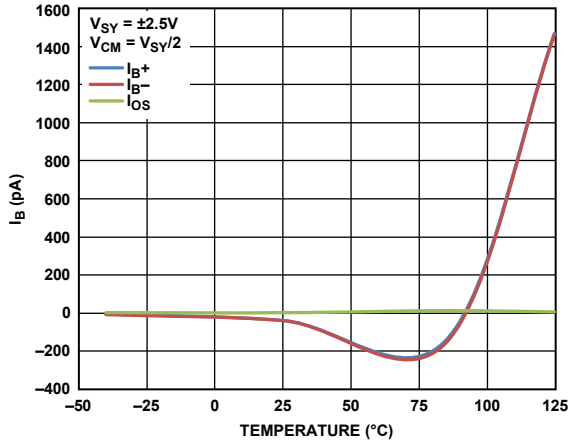


Figure 16. Input Bias Current (I_B) vs. Temperature, $V_{SY} = \pm 2.5V$



Figure 19. Input Bias Current (I_B) vs. Temperature, $V_{SY} = \pm 27.5V$

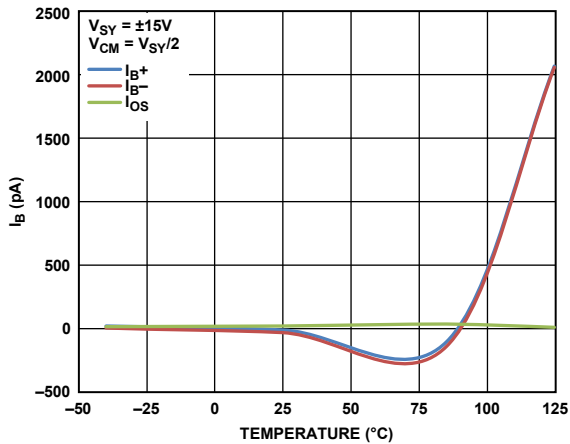


Figure 17. Input Bias Current (I_B) vs. Temperature, $V_{SY} = \pm 15V$

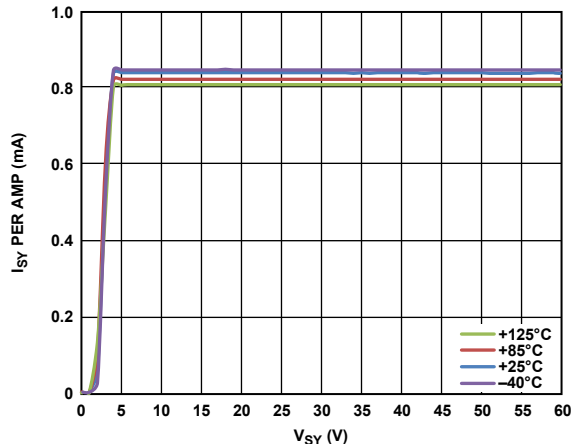


Figure 20. Supply Current (I_{SY}) per Amplifier vs. Supply Voltage (V_{SY})

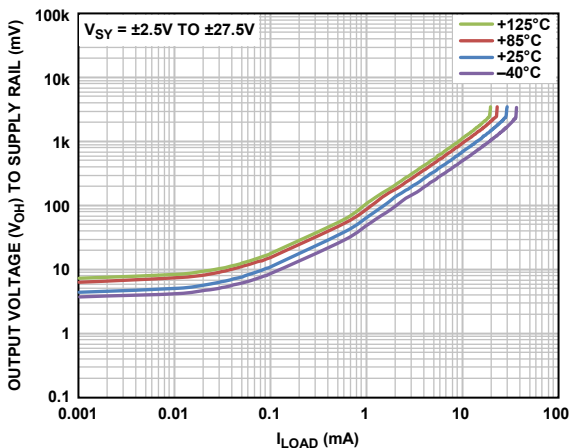


Figure 18. Output Voltage High (V_{OH}) to Supply Rail vs. Load Current (I_{LOAD})

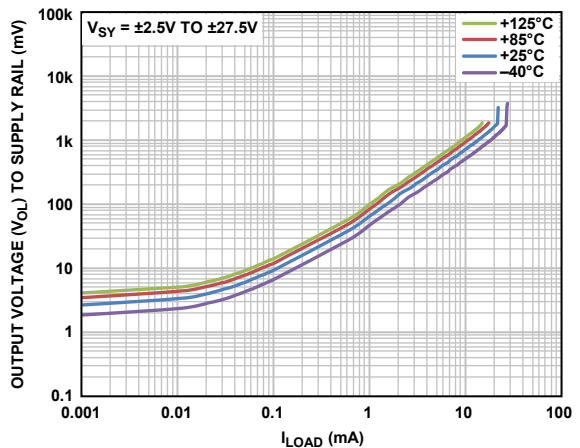
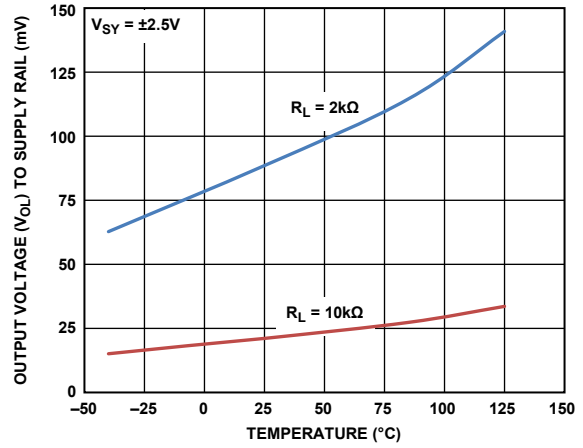


Figure 21. Output Voltage Low (V_{OL}) to Supply Rail vs. Load Current (I_{LOAD})



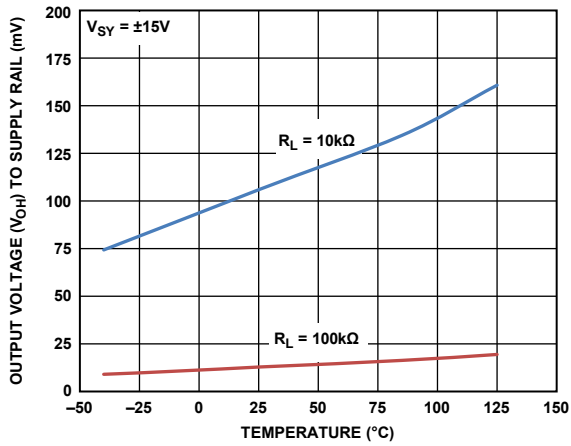
13168-018

Figure 22. Output Voltage High (V_{OH}) to Supply Rail vs. Temperature, $V_{SY} = \pm 2.5V$



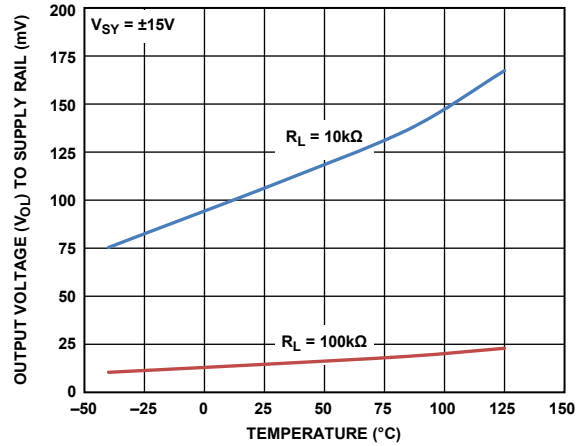
13168-021

Figure 25. Output Voltage Low (V_{OL}) to Supply Rail vs. Temperature, $V_{SY} = \pm 2.5V$



13168-019

Figure 23. Output Voltage High (V_{OH}) to Supply Rail vs. Temperature, $V_{SY} = \pm 15V$



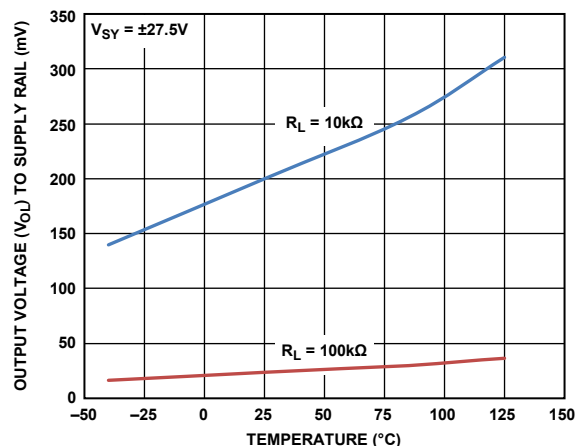
13168-022

Figure 26. Output Voltage Low (V_{OL}) to Supply Rail vs. Temperature, $V_{SY} = \pm 15V$



13168-020

Figure 24. Output Voltage High (V_{OH}) to Supply Rail vs. Temperature, $V_{SY} = \pm 27.5V$



13168-023

Figure 27. Output Voltage Low (V_{OL}) to Supply Rail vs. Temperature, $V_{SY} = \pm 27.5V$



Figure 28. CMRR vs. Frequency

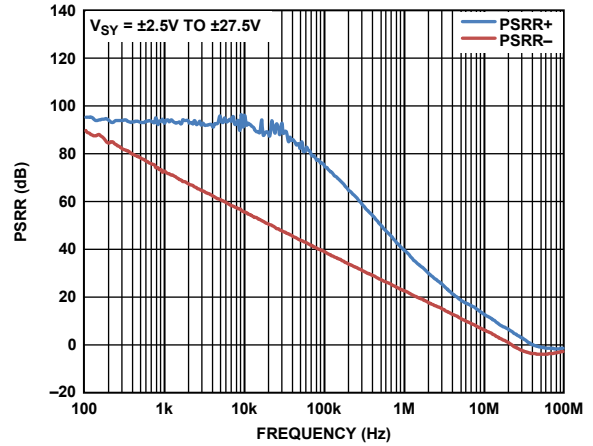


Figure 31. PSRR vs. Frequency

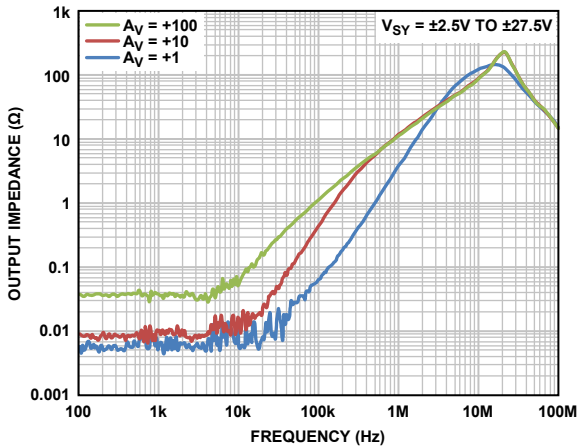


Figure 29. Closed-Loop Output Impedance vs. Frequency

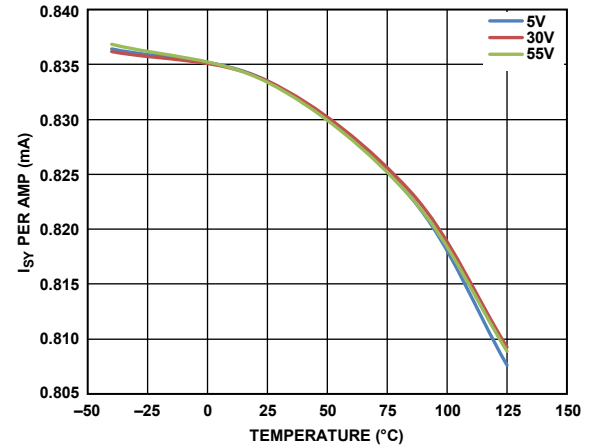


Figure 32. Supply Current (I_{SY}) per Amplifier vs. Temperature

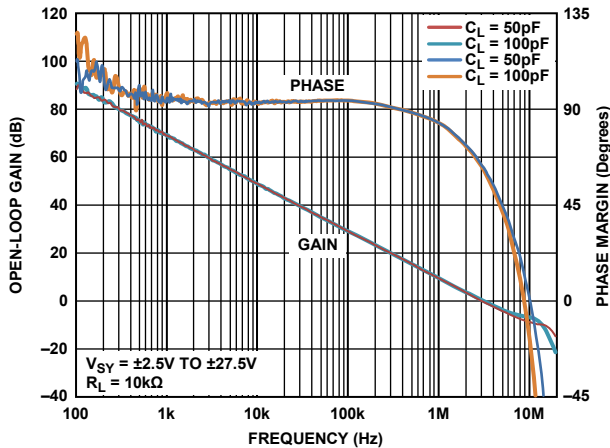


Figure 30. Open-Loop Gain and Phase Margin vs. Frequency

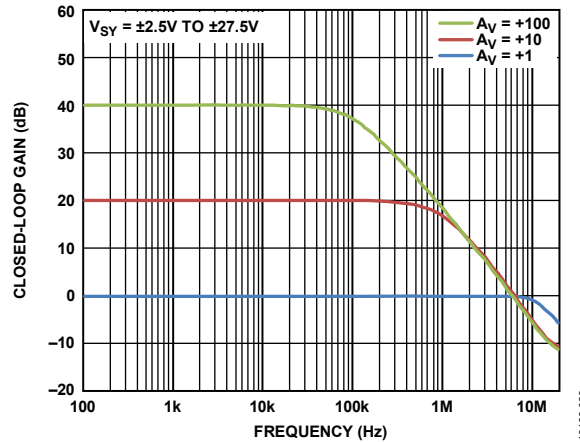


Figure 33. Closed-Loop Gain vs. Frequency



Figure 34. Large Signal Transient Response, $V_{SY} = \pm 2.5\text{ V}$

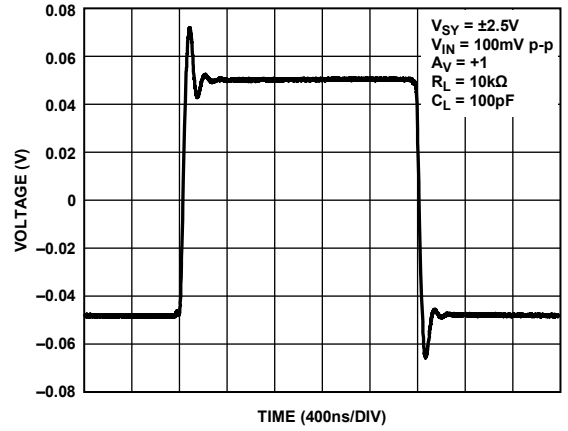


Figure 37. Small Signal Transient Response, $V_{SY} = \pm 2.5\text{ V}$

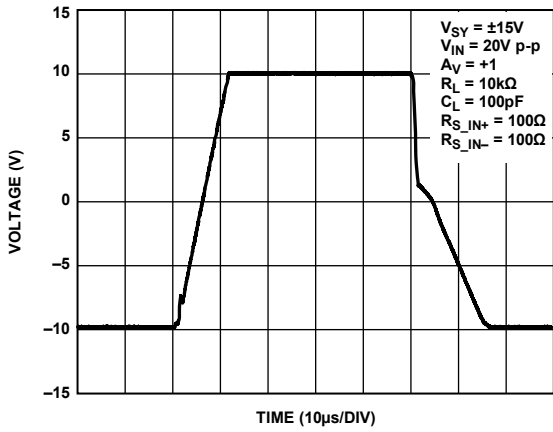


Figure 35. Large Signal Transient Response, $V_{SY} = \pm 15\text{ V}$

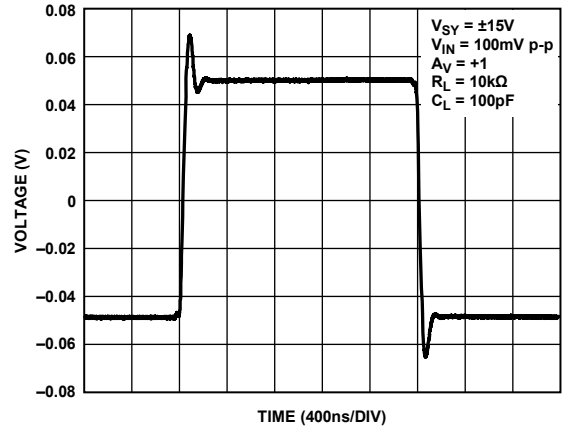


Figure 38. Small Signal Transient Response, $V_{SY} = \pm 15\text{ V}$

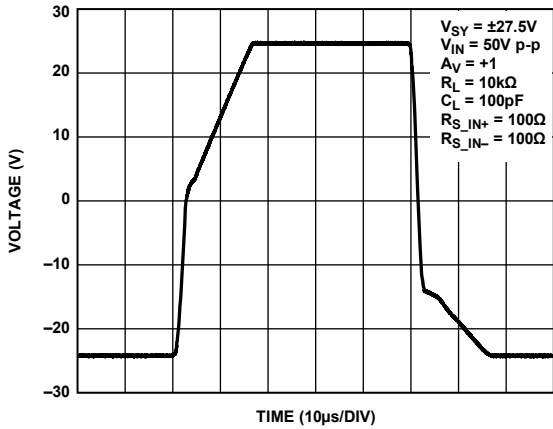


Figure 36. Large Signal Transient Response, $V_{SY} = \pm 27.5\text{ V}$

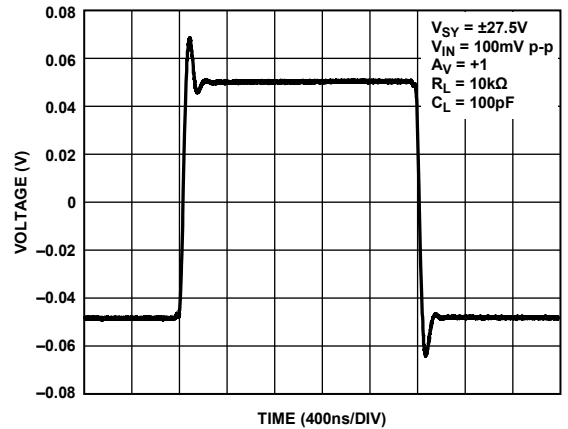


Figure 39. Small Signal Transient Response, $V_{SY} = \pm 27.5\text{ V}$



Figure 40. Small Signal Overshoot vs. Load Capacitance, $V_{SY} = \pm 2.5 V$

13168-040

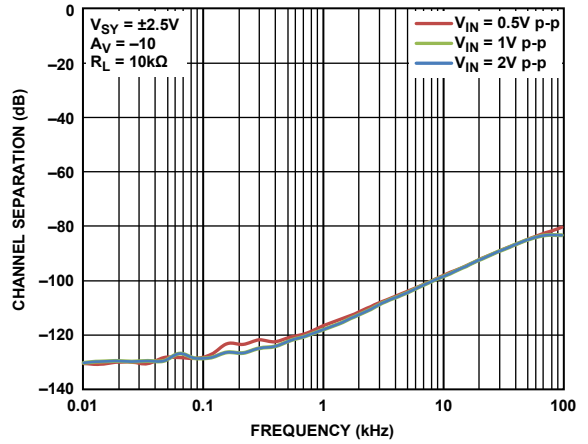


Figure 43. Channel Separation vs. Frequency, $V_{SY} = \pm 2.5 V$

13168-043

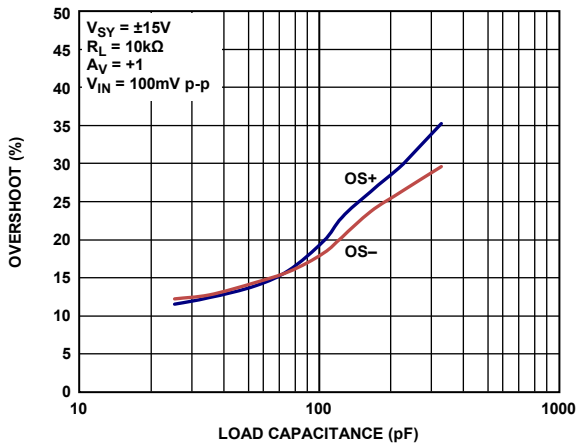


Figure 41. Small Signal Overshoot vs. Load Capacitance, $V_{SY} = \pm 15 V$

13168-041

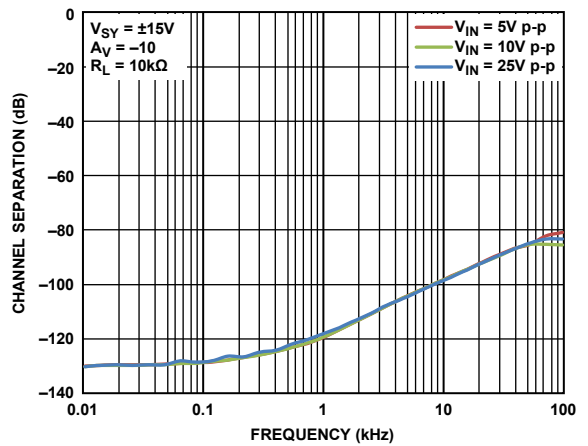


Figure 44. Channel Separation vs. Frequency, $V_{SY} = \pm 15 V$

13168-044

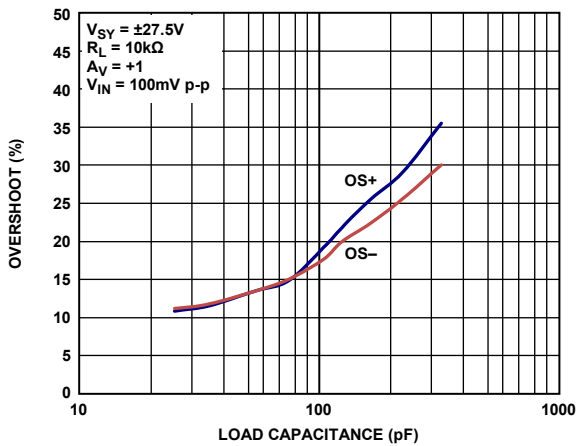


Figure 42. Small Signal Overshoot vs. Load Capacitance, $V_{SY} = \pm 27.5 V$

13168-042

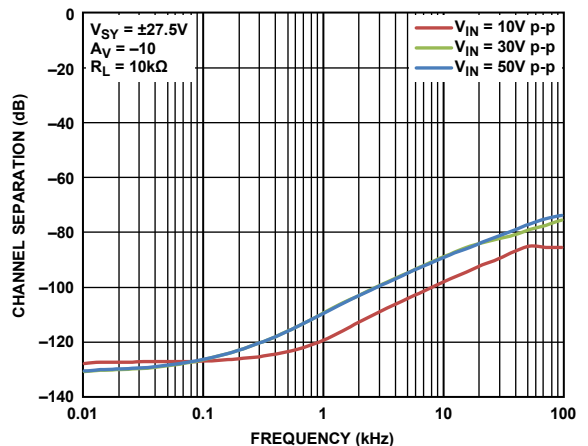


Figure 45. Channel Separation vs. Frequency, $V_{SY} = \pm 27.5 V$

13168-045

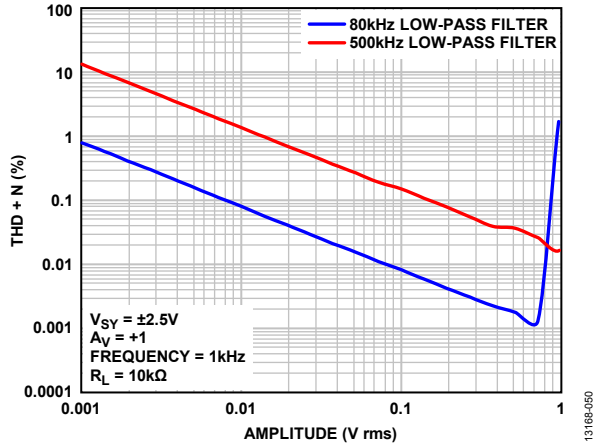


Figure 46. THD + N vs. Amplitude, $V_{SY} = \pm 2.5 V$

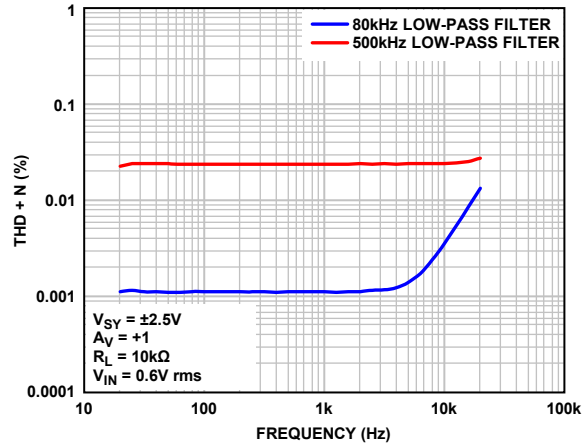


Figure 49. THD + N vs. Frequency, $V_{SY} = \pm 2.5 V$

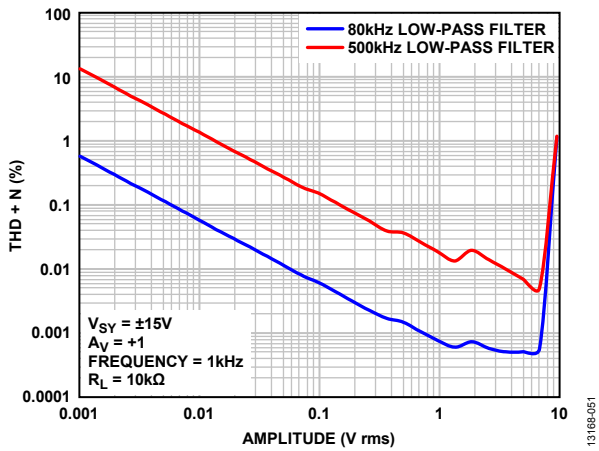


Figure 47. THD + N vs. Amplitude, $V_{SY} = \pm 15 V$

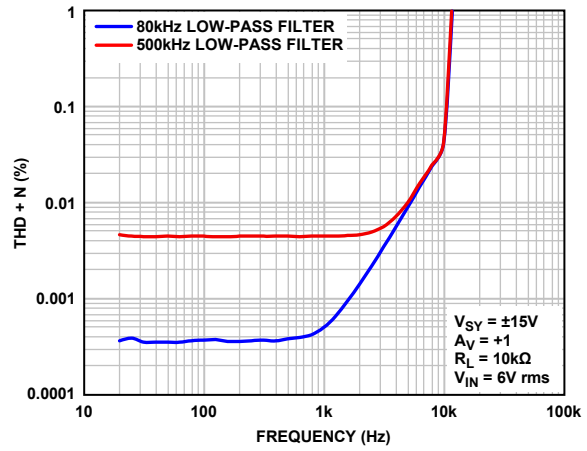


Figure 50. THD + N vs. Frequency, $V_{SY} = \pm 15 V$

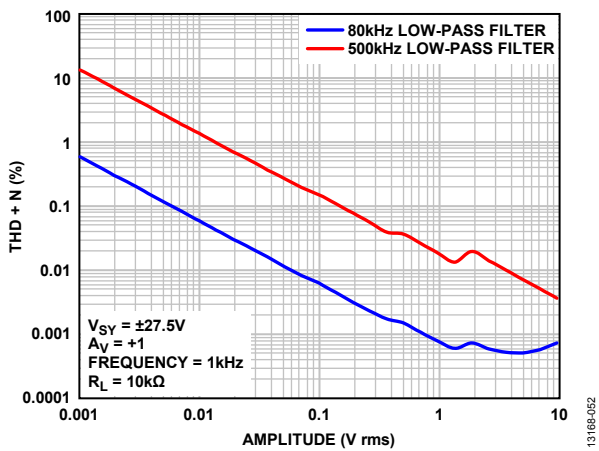


Figure 48. THD + N vs. Amplitude, $V_{SY} = \pm 27.5 V$

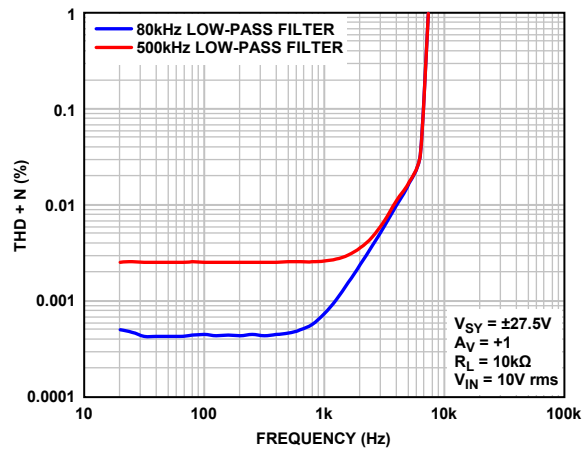


Figure 51. THD + N vs. Frequency, $V_{SY} = \pm 27.5 V$



Figure 52. Positive Overload Recovery, $V_{SY} = \pm 2.5\text{ V}$

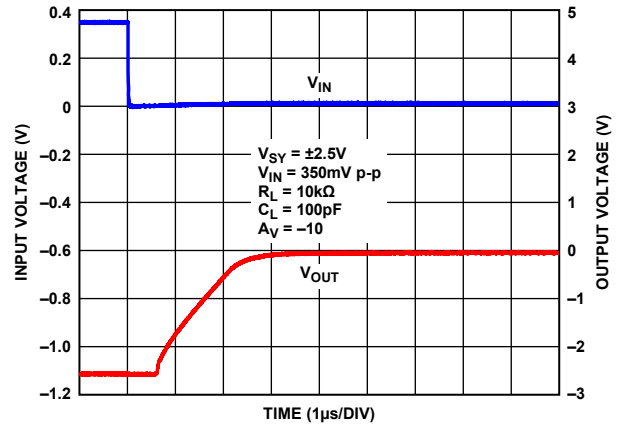


Figure 55. Negative Overload Recovery, $V_{SY} = \pm 2.5\text{ V}$

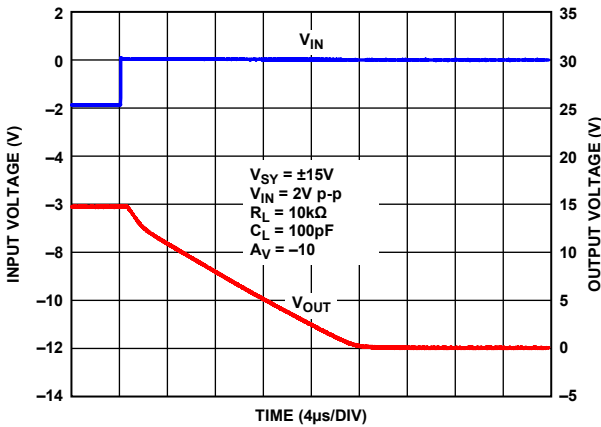


Figure 53. Positive Overload Recovery, $V_{SY} = \pm 15\text{ V}$

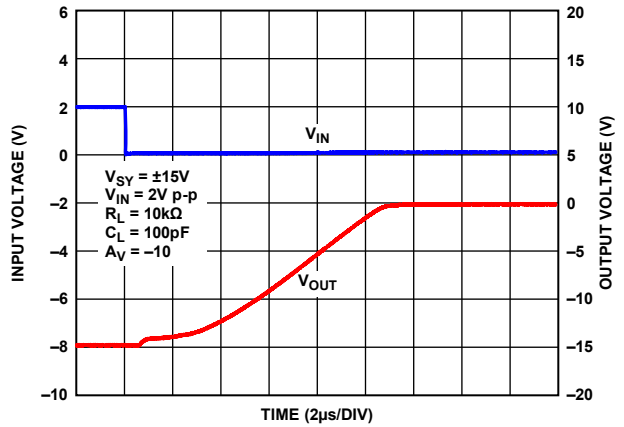


Figure 56. Negative Overload Recovery, $V_{SY} = \pm 15\text{ V}$

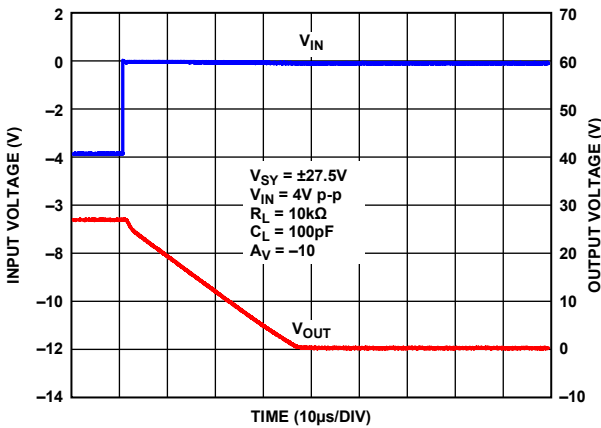


Figure 54. Positive Overload Recovery, $V_{SY} = \pm 27.5\text{ V}$

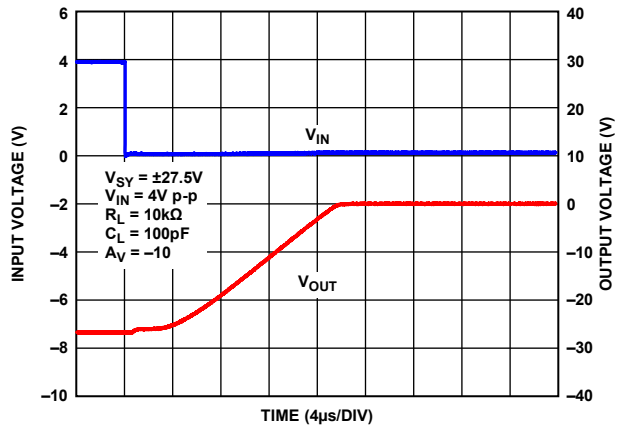


Figure 57. Negative Overload Recovery, $V_{SY} = \pm 27.5\text{ V}$

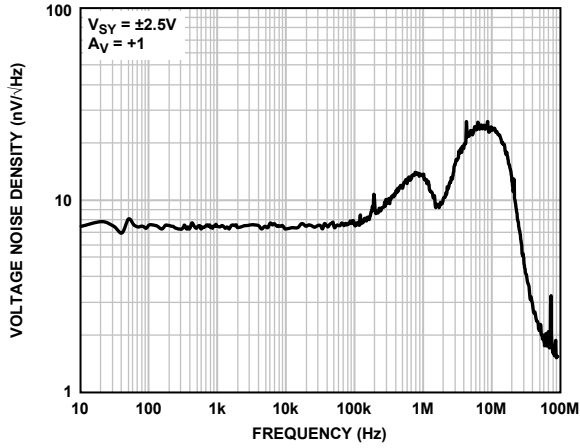


Figure 58. Voltage Noise Density, $V_{SY} = \pm 2.5 V$

13168-062

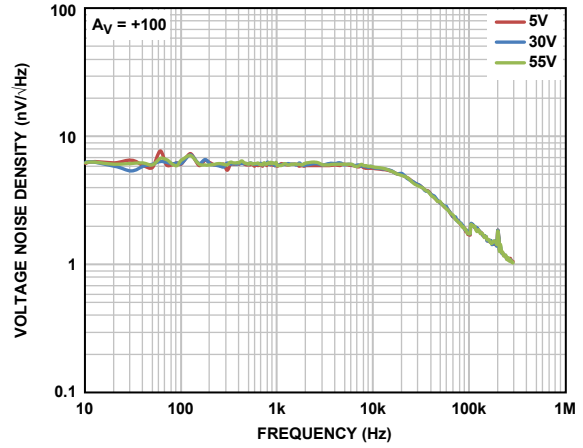


Figure 61. Voltage Noise Density, $A_V = +100$

13168-065

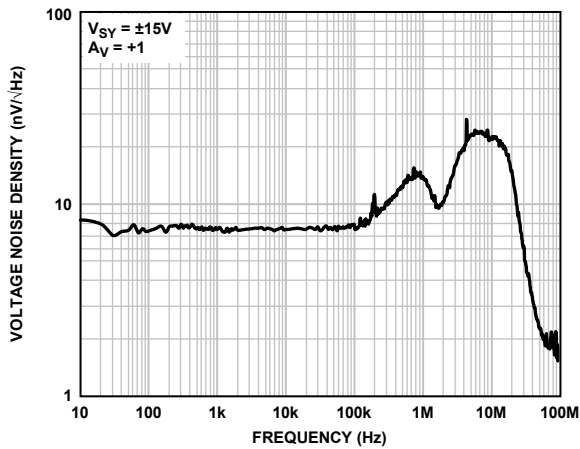


Figure 59. Voltage Noise Density, $V_{SY} = \pm 15 V$

13168-063

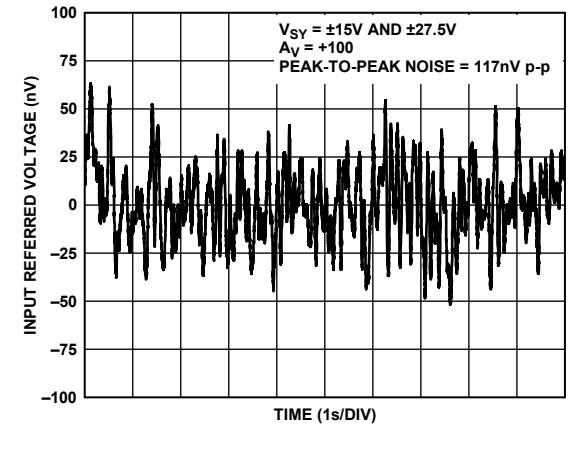


Figure 62. 0.1 Hz to 10 Hz Noise

13168-066

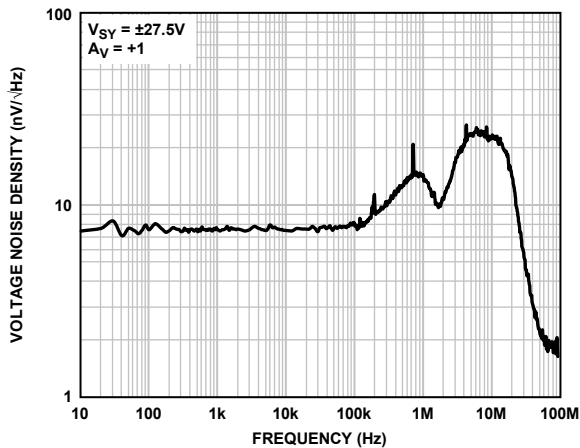


Figure 60. Voltage Noise Density, $V_{SY} = \pm 27.5 V$

13168-064

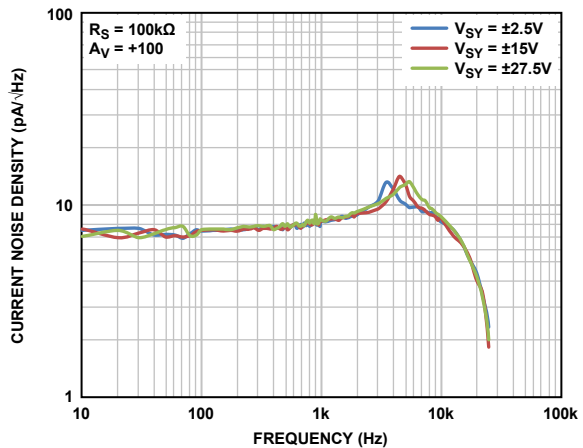


Figure 63. Current Noise Density

13168-067

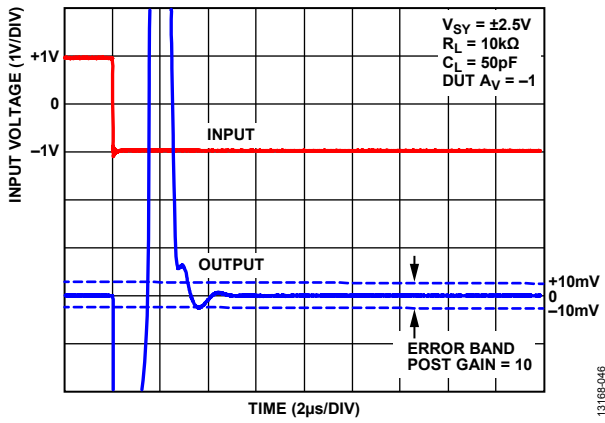


Figure 64. Negative Settling Time to 0.1%, $V_{SY} = \pm 2.5V$



Figure 67. Positive Settling Time to 0.1%, $V_{SY} = \pm 2.5V$



Figure 65. Negative Settling Time to 0.1%, $V_{SY} = \pm 15V$ and $\pm 27.5V$



Figure 68. Positive Settling Time to 0.1%, $V_{SY} = \pm 15V$ and $\pm 27.5V$



Figure 66. Output Voltage Swing vs. Frequency

APPLICATIONS INFORMATION

The ADA4522-2 is a dual, ultralow noise, high voltage, zero drift, rail-to-rail output operational amplifier. It features a patented chopping technique that offers an ultralow input offset voltage of 5 μV and an input offset voltage drift of 22 $\text{nV}/^\circ\text{C}$ maximum. Offset voltage errors due to common-mode voltage swings and power supply variations are also corrected by the chopping technique, resulting in a superb typical CMRR figure of 160 dB and a PSRR figure of 160 dB at a 30 V supply voltage.

The ADA4522-2 has wide operating voltages from $\pm 2.25\text{ V}$ (or 4.5 V) to $\pm 27.5\text{ V}$ (or 55 V). It is a single supply amplifier, where its input voltage range includes the lower supply rail. It also offers low broadband noise of 5.8 $\text{nV}/\sqrt{\text{Hz}}$ (at $f = 1\text{ kHz}$, $A_V = 100$) and reduced $1/f$ noise component. These features are ideal for the amplification of low level signals in high precision applications. A few examples of such applications are weigh scales, high precision current sensing, high voltage buffers, signal conditioning for temperature sensors, among others.

THEORY OF OPERATION

Figure 69 shows the ADA4522-2 architecture block diagram. It consists of an input EMI filter and clamp circuitry, three gain stages (G_{m1} , G_{m2} , and G_{m3}), input and output chopping networks (CHOP_{IN} and CHOP_{OUT}), a clock generator, offset and ripple correction loop circuitry, frequency compensation capacitors (C_1 , C_2 , and C_3), and thermal shutdown circuitry.

An EMI filter and clamp circuit is implemented at the input front end to protect the internal circuitry against electrostatic discharge (ESD) stresses and high voltage transients. The ability of the amplifier to reject EMI is explained in detail in the EMI Rejection Ratio section.

CHOP_{IN} and CHOP_{OUT} are controlled by a clock generator and operate at 4.8 MHz. The input baseband signal is initially modulated by CHOP_{IN} . Next, CHOP_{OUT} demodulates the input signal and modulates the millivolt-level input offset voltage and $1/f$ noise of the input transconductance amplifier, G_{m1} , to the chopping frequency at 4.8 MHz. The chopping networks remove the low frequency errors, but in return, the networks introduce chopping artifacts at the chopping frequency. Therefore, a patented offset and ripple correction loop, operating at 800 kHz, is used. This frequency is the switching frequency of the amplifier. This patented circuitry reduces chopping artifacts, allowing the ADA4522-2 to have a high chopping frequency with minimal artifacts.

The thermal shutdown circuit shuts down the circuit when the die is overheated; this is explained further in the Thermal Shutdown section.

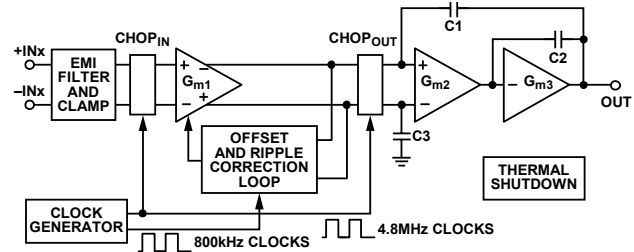


Figure 69. ADA4522-2 Block Diagram

ON-CHIP INPUT EMI FILTER AND CLAMP CIRCUIT

Figure 70 shows the input EMI filter and clamp circuit. The ADA4522-2 has internal ESD protection diodes (D_1 , D_2 , D_3 , and D_4) that are connected between the inputs and each supply rail. These diodes protect the input transistors in the event of electrostatic discharge and are reverse biased during normal operation. This protection scheme allows voltages as high as approximately 300 mV beyond the rails to be applied at the input of either terminal without causing permanent damage. See Table 5 in the Absolute Maximum Ratings section for more information.

The EMI filter is composed of two 200 Ω input series resistors (R_{S1} and R_{S2}), two common-mode capacitors ($C_{\text{CM}1}$ and $C_{\text{CM}2}$), and a differential capacitor (C_{DM}). These RC networks set the -3 dB low-pass cutoff frequencies at 50 MHz for common-mode signals, and at 33 MHz for differential signals. After the EMI filter, back to back diodes (D_5 and D_6) are added to protect internal circuit devices from high voltage input transients. Each diode has about 1 V of forward turn on voltage. See the Large Signal Transient Response section for more information on the effect of high voltage input transient on the ADA4522-2.

As specified in the Absolute Maximum Ratings table (Table 5), the maximum input differential voltage is limited to $\pm 5\text{ V}$. If more than $\pm 5\text{ V}$ is applied, a continuous current larger than $\pm 10\text{ mA}$ flows through one of the back to back diodes. This compromises long term reliability and can cause permanent damage to the device.

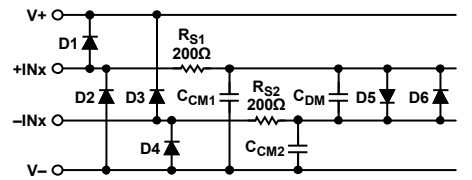


Figure 70. Input EMI Filter and Clamp Circuit

THERMAL SHUTDOWN

The ADA4522-2 has internal thermal shutdown circuitry for each channel of the amplifier. The thermal shutdown circuitry prevents internal devices from being damaged by an overheat condition in the die. Overheat can occur due to a high ambient temperature, a high supply voltage, and/or high output currents. As specified in Table 5, care must be taken to maintain the junction temperature below 150°C.

Two conditions affect junction temperature (T_J): the total power dissipation of the device (P_D) and the ambient temperature surrounding the package (T_A). Use the following equation to estimate the approximate junction temperature:

$$T_J = P_D \times \theta_{JA} + T_A \quad (1)$$

where θ_{JA} is the thermal resistance between the die and the ambient environment, as shown in Table 6.

The total power dissipation is the sum of quiescent power of the device and the power required to drive a load for all channels of an amplifier. The power dissipation per amplifier ($P_{D_PER_AMP}$) for sourcing a load is shown in Equation 2.

$$P_{D_PER_AMP} = (V_{SY+} - V_{SY-}) \times I_{SY_PER_AMP} + I_{OUT} \times (V_{SY+} - V_{OUT}) \quad (2)$$

When sinking current, replace $(V_{SY+} - V_{OUT})$ in Equation 2 with $(V_{OUT} - V_{SY-})$.

Also, take note to include the power dissipation of both channels of the amplifier when calculating the total power dissipation for the ADA4522-2.

The thermal shutdown circuitry does not guarantee that the device is to be free of permanent damage if the junction temperature exceeds 150°C. However, the internal thermal shutdown function may help avoid permanent damage or reduce the degree of damage. Each amplifier channel has thermal shutdown circuitry, composed of a temperature sensor with hysteresis.

As soon as the junction temperature reaches 190°C, the thermal shutdown circuitry shuts down the amplifier. Note that either one of the two thermal shutdown circuitries are activated; this activation disables the channel. When the amplifier is disabled, the output becomes open state and the quiescent current of the channel decreases to 0.1 mA. When the junction temperature cools down to 160°C, the thermal shutdown circuitry enables the amplifier and the quiescent current increases to its typical value.

When overheating in the die is caused by an undesirable excess amount of output current, the thermal shutdown circuit repeats its function. The junction temperature keeps increasing until it reaches 190°C and one of the channels is disabled. Then, the junction temperature cools down until it reaches 160°C, and the channel is enabled again. The process then repeats.

INPUT PROTECTION

When either input of the ADA4522-2 exceeds one of the supply rails by more than 300 mV, the ESD diodes mentioned in the On-Chip Input EMI Filter and Clamp Circuit section become forward-biased and large amounts of current begin to flow through them. Without current limiting, this excessive fault current causes permanent damage to the device. If the inputs are expected to be subject to overvoltage conditions, insert a resistor in series with each input to limit the input current to ± 10 mA maximum. However, consider the resistor thermal noise effect on the entire circuit.

At ± 15 V supply voltage, the broadband voltage noise of the ADA4522-2 is approximately 7.3 nV/ $\sqrt{\text{Hz}}$ (at unity gain), and a 1 k Ω resistor has thermal noise of 4 nV/ $\sqrt{\text{Hz}}$. Adding a 1 k Ω resistor increases the total noise to 8.3 nV/ $\sqrt{\text{Hz}}$.

SINGLE-SUPPLY AND RAIL-TO-RAIL OUTPUT

The ADA4522-2 is a single-supply amplifier, where its input voltage range includes the lower supply rail. This is ideal for applications where the input common-mode voltage is at the lower supply rail, for example, ground sensing. On the other hand, the amplifier output is rail-to-rail. Figure 71 shows the input and output waveforms of the ADA4522-2 configured as a unity-gain buffer with a supply voltage of ± 15 V. With an input voltage of ± 15 V, the low output voltage tracks the input voltage, whereas the high output swing clamps/distorts when the input goes out of the input voltage range ($-15 \text{ V} \leq \text{IVR} \leq +13.5 \text{ V}$). However, the device does not exhibit phase reversal.

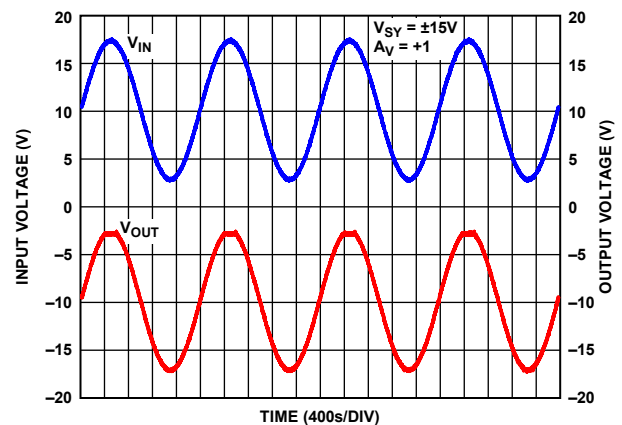


Figure 71. No Phase Reversal

13186-070

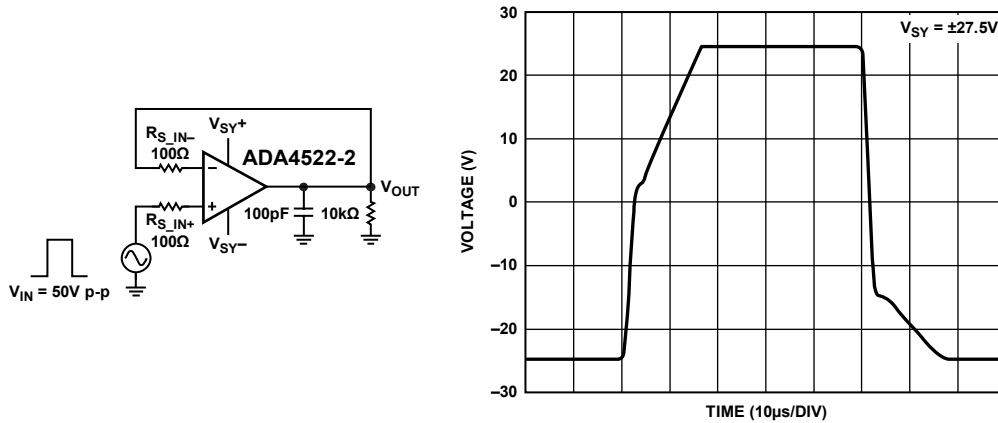


Figure 72. Large Signal Transient Response Example

LARGE SIGNAL TRANSIENT RESPONSE

When the ADA4522-2 is configured in a closed-loop configuration with a large input transient (for example, a step input voltage), the internal back to back diodes may turn on. Consider a case where the amplifier is in unity-gain configuration with a step input waveform. This is shown in Figure 72.

The noninverting input is driven by an input signal source and the inverting input is driven by the output of the amplifier. The maximum amplifier output current depends on the input step function and the external source resistance at the input terminals of the amplifier.

Case 1

If the external source resistance is low (for example, 100 Ω in Figure 72) or if the input step function is large, the maximum amplifier output current is limited to the output short-circuit current as specified in the Specifications section. The maximum differential voltage between the input signal and the amplifier output is then limited by the maximum amplifier output current multiplied by the total input resistance (internal and external) and the turn on voltage of the back to back diode (see Figure 70 for the input EMI filter and clamp circuit architecture). When the noninverting input voltage changes with a step signal, the inverting input voltage (and, therefore, the output voltage) follows the change quickly until it reaches the maximum differential voltage between the input signal and amplifier output possible. The inverting input voltage then starts slewing with the slew rate specified in the Specifications section until it reaches its desired output. Therefore, as seen in Figure 72, there are two distinctive sections of the rising and falling edge of the output waveform. With this test condition, the amount and duration of the input/output current is limited and, therefore, does not damage the amplifier.

Case 2

If the external source resistance is high or if the input step function is small, the maximum output current is limited to the instantaneous difference between the input signal and amplifier output voltage (which is the change in the step function) divided by the source resistance. This maximum output current is less than

the amplifier output short-circuit current. The maximum differential voltage between the input signal and the amplifier output is then equal to the step function. The output voltage slews until it reaches its desired output.

Therefore, if desired, reduce the input current by adding a larger external resistor between the signal source and the noninverting input. Similarly, to reduce output current, add an external resistor to the feedback loop between the inverting input and output. This large signal transient response issue is typically not a problem when the amplifier is configured in closed-loop gain, where the input signal source is usually much smaller and the gain and feedback resistors limit the current.

Back to back diodes are also implemented in many other amplifiers; these amplifiers show similar slewing behavior.

NOISE CONSIDERATIONS

1/f Noise

1/f noise, also known as pink noise or flicker noise, is inherent in semiconductor devices and increases as frequency decreases. At a low frequency, 1/f noise is a major noise contributor and causes a significant output voltage offset when amplified by the noise gain of the circuit. However, because the low frequency 1/f noise appears as a slow varying offset to the ADA4522-2, it is effectively reduced by the chopping technique. This allows the ADA4522-2 to have a much lower noise at dc and low frequency in comparison to standard low noise amplifiers that are susceptible to 1/f noise. Figure 62 shows the 0.1 Hz to 10 Hz noise to be only 117 nV p-p of noise.

Source Resistance

The ADA4522-2 is one of the lowest noise high voltage zero drift amplifiers with 5.8 nV/√Hz of broadband noise at 1 kHz ($A_V = 100$). Therefore, it is important to consider the input source resistance of choice to maintain a total low noise. The total input referred broadband noise (e_N total) from any amplifier is primarily a function of three types of noise: input voltage noise, input current noise, and thermal (Johnson) noise from the external resistors.

These uncorrelated noise sources can be summed up in a root sum squared (rss) manner by using the following equation:

$$e_{N \text{ total}} = [e_N^2 + 4 kTR_S + (i_N \times R_S)^2]^{1/2}$$

where:

e_N is the input voltage noise density of the amplifier ($V/\sqrt{\text{Hz}}$).

k is the Boltzmann's constant (1.38×10^{-23} J/K).

T is the temperature in Kelvin (K).

R_S is the total input source resistance (Ω).

i_N is the input current noise density of the amplifier ($A/\sqrt{\text{Hz}}$).

The total equivalent rms noise over a specific bandwidth is expressed as

$$e_{N \text{ RMS}} = e_{N \text{ total}} \sqrt{BW}$$

where BW is the bandwidth in hertz.

This analysis is valid for broadband noise calculation up to a decade before the switching frequency. If the bandwidth of concern includes the switching frequency, more complicated calculations must be made to include the effect of the increase in noise at the switching frequency.

With a low source resistance of $R_S < 1 \text{ k}\Omega$, the voltage noise of the amplifier dominates. As the source resistance increases, the thermal noise of R_S dominates. As the source resistance further increases, where $R_S > 50 \text{ k}\Omega$, the current noise becomes the main contributor of the total input noise.

Residual Ripple

As shown in Figure 58, Figure 59, and Figure 60, the ADA4522-2 has a flat noise spectrum density at lower frequencies and exhibits spectrum density bumps and peaks at higher frequencies.

The largest noise bump is centered at 6 MHz; this is due to the decrease in the input gain at higher frequencies. This is a typical phenomenon and can also be seen in other amplifiers. In addition to the noise bump, a sharp peak due to the chopping networks is seen at 4.8 MHz. However, this magnitude is significantly reduced by the offset and ripple correction loop. Its magnitude may be different with different amplifier units or with different circuitries around the amplifier. This peak can potentially be hidden by the noise bump and, therefore, may not be detected.

The offset and ripple correction loop, designed to reduce the 4.8 MHz switching artifact, also creates a noise bump centered at 800 kHz and a noise peak on top of this noise bump. Although the magnitude of the bump is mostly constant, the magnitude of the 800 kHz peak is different from unit to unit. Some units may not exhibit the 800 kHz noise peak, however, for other units, peaks occur at multiple integrals of 800 kHz, such as 1.6 MHz or 2.4 MHz.

These noise peaks, albeit small in magnitude, can be significant when the amplifier has a closed-loop frequency that is higher than the chopping frequency. To suppress the noise spike to a desired level, one can either configure the amplifier in high gain configuration or apply a post filter at the output of the amplifier.

Figure 73 shows the voltage noise density of the ADA4522-2 in different gain configurations. Note that the higher the gain, the lower the available bandwidth is. The earlier bandwidth roll-off effectively filters out the higher noise spectrum.

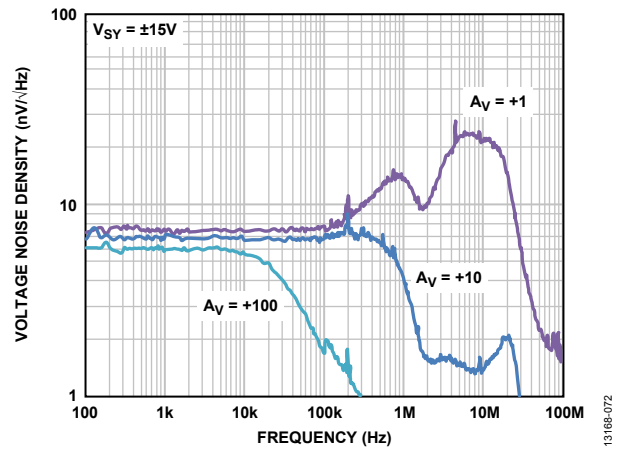


Figure 73. Voltage Noise Density with Various Gains

Figure 74 shows the voltage noise density of the ADA4522-2 without and with post filters at different frequencies. The post filter serves to roll off the bandwidth before the switching frequency. In this example, the noise peak at 800 kHz is about 38 nV/√Hz. With a post filter at 80 kHz, the noise peak is reduced to 4.1 nV/√Hz. With a post filter at 8 kHz, the noise peak is lower than the noise floor and cannot be detected.

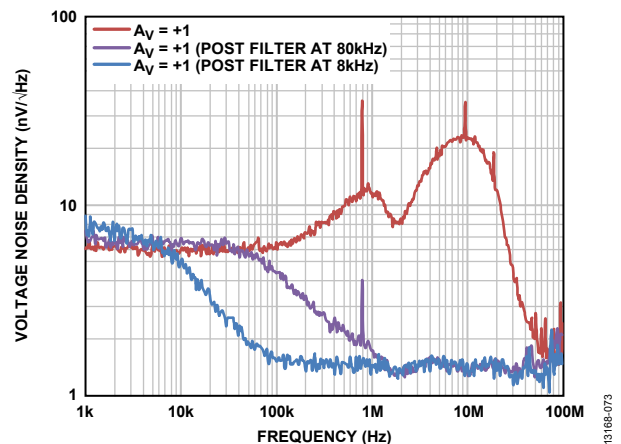


Figure 74. Voltage Noise Density with Post Filters

Current Noise Density

Figure 75 shows the current noise density of the ADA4522-2 at unity gain. At 1 kHz, current noise density is about 1.3 pA/√Hz. Current noise density is determined by measuring the voltage noise due to current noise flowing through a resistor. Due to the low current noise density of the amplifier, the voltage noise is usually measured with a high value resistor; in this case, a 100 kΩ source resistor is used. However, the source resistor interacts with the input capacitance of the amplifier and board, causing bandwidth to roll off. Note that Figure 75 shows the current noise density rolling off much earlier than the unity-gain bandwidth; this is expected.

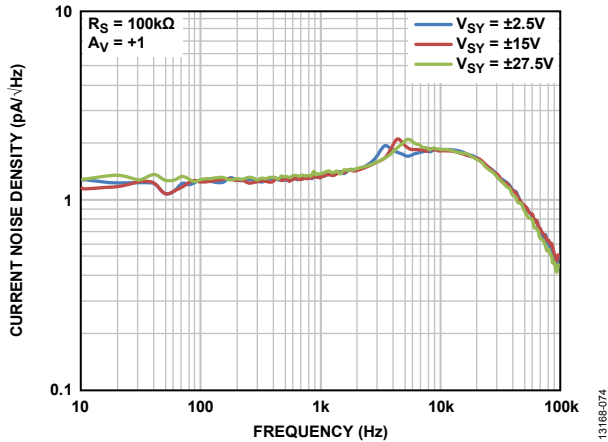


Figure 75. Current Noise Density at Gain = 1

EMI REJECTION RATIO

Circuit performance is often adversely affected by high frequency EMI. When the signal strength is low and transmission lines are long, an op amp must accurately amplify the input signals. However, all op amp pins—the noninverting input, inverting input, positive supply, negative supply, and output pins—are susceptible to EMI signals. These high frequency signals are coupled into an op amp by various means, such as conduction, near field radiation, or far field radiation. For example, wires and PCB traces can act as antennas and pick up high frequency EMI signals.

Amplifiers do not amplify EMI or RF signals due to their relatively low bandwidth. However, due to the nonlinearities of the input devices, op amps can rectify these out of band signals. When these high frequency signals are rectified, they appear as a dc offset at the output.

The ADA4522-2 has integrated EMI filters at its input stage. To describe the ability of the ADA4522-2 to perform as intended in the presence of electromagnetic energy, the electromagnetic interference rejection ratio (EMIRR) of the noninverting pin is specified in Table 2, Table 3, and Table 4 of the Specifications section. A mathematical method of measuring EMIRR is defined as follows:

$$EMIRR = 20\log(V_{IN_PEAK}/\Delta V_{OS})$$

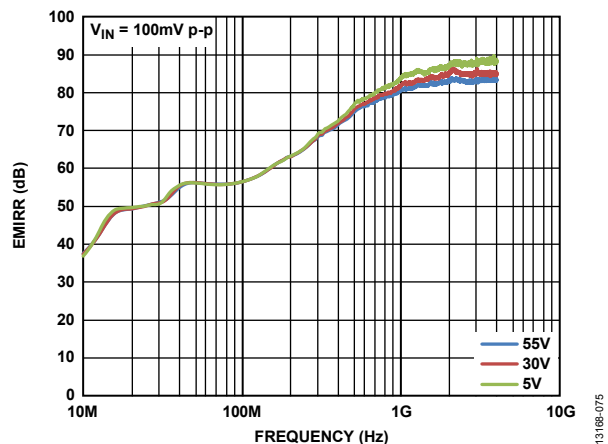


Figure 76. EMIRR vs. Frequency

CAPACITIVE LOAD STABILITY

The ADA4522-2 can safely drive capacitive loads of up to 250 pF in any configuration. As with most amplifiers, driving larger capacitive loads than specified may cause excessive overshoot and ringing, or even oscillation. A heavy capacitive load reduces phase margin and causes the amplifier frequency response to peak. Peaking corresponds to overshooting or ringing in the time domain. Therefore, it is recommended that external compensation be used if the ADA4522-2 must drive a load exceeding 250 pF. This compensation is particularly important in the unity-gain configuration, which is the worst case for stability.

A quick and easy way to stabilize the op amp for capacitive load drive is by adding a series resistor, RISO, between the amplifier output terminal and the load capacitance, as shown in Figure 77. RISO isolates the amplifier output and feedback network from the capacitive load. However, with this compensation scheme, the output impedance as seen by the load increases, and this reduces gain accuracy.

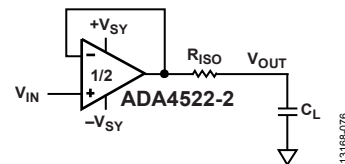


Figure 77. Stability Compensation with Isolating Resistor, RISO

Figure 78 shows the effect on overshoot with different values of RISO.

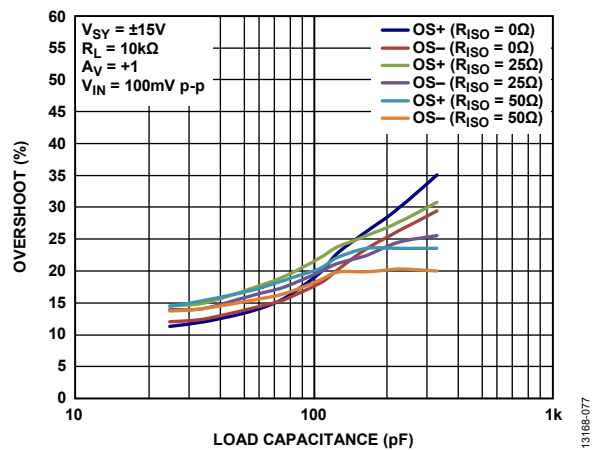


Figure 78. Small Signal Overshoot vs. Load Capacitance with Various Output Isolating Resistors

SINGLE-SUPPLY INSTRUMENTATION AMPLIFIER

The extremely low offset voltage and drift, high open-loop gain, high common-mode rejection, and high power supply rejection of the ADA4522-2 make it an excellent op amp choice as a discrete, single-supply instrumentation amplifier.

Figure 79 shows the classic 3-op-amp instrumentation amplifier using the ADA4522-2. The key to high CMRR for the instrumentation amplifier are resistors that are well matched for both the resistive ratio and relative drift. For true difference amplification, matching of the resistor ratio is very important, where $R5/R2 = R6/R4$. The resistors are important in determining the performance over manufacturing tolerances, time, and temperature. Assuming a perfect unity-gain difference amplifier with infinite common-mode rejection, a 1% tolerance resistor matching results in only 34 dB of common-mode rejection. Therefore, at least 0.01% or better resistors are recommended.



Figure 79. Discrete 3-Op Amp Instrumentation Amplifier

To build a discrete instrumentation amplifier with external resistors without compromising on noise, pay close attention to the resistor values chosen. R_{G1} and R_{G2} each have thermal noise that is amplified by the total noise gain of the instrumentation amplifier and, therefore, must be chosen sufficiently low to reduce thermal noise contribution at the output while still providing an accurate measurement. Table 8 shows the external resistors noise contribution referred to the output (RTO).

Table 8. Thermal Noise Contribution Example

Resistor	Value (kΩ)	Resistor Thermal Noise (nV/√Hz)	Thermal Noise RTO (nV/√Hz)
R_{G1}	0.4	2.57	128.30
R_{G2}	0.4	2.57	128.30
R1	10	12.83	25.66
R2	10	12.83	25.66
R3	10	12.83	25.66
R4	10	12.83	25.66
R5	20	18.14	18.14
R6	20	18.14	18.14

Note that A1 and A2 have a high gain of $1 + R1/R_{G1}$. Therefore, use a high precision, low offset voltage and low noise amplifier for A1 and A2, such as the ADA4522-2. On the other hand, A3 operates at a much lower gain and has a different set of op amp requirements. Its input noise, referred to the overall instrumentation amplifier input, is divided by the first stage gain and is not

as important. Note that the input offset voltage and the input voltage noise of the amplifiers are also amplified by the overall noise gain.

Understanding how noise impacts a discrete instrumentation amplifier or a difference amplifier (the second stage of a 3-op-amp instrumentation amplifier) is important, because they are commonly used in many different applications. The Load Cell/Strain Gage Sensor Signal Conditioning section and the Precision Low-Side Current Shunt Sensor section show the ADA4522-2 used as a discrete instrumentation or difference amplifier in an application.

LOAD CELL/STRAIN GAGE SENSOR SIGNAL CONDITIONING

The ADA4522-2, with its ultralow offset, drift, and noise, is well suited to signal condition low level sensor output with high gain and accuracy. A weigh scale/load cell is an example of an application with such requirements. Figure 80 shows a configuration for a single supply, precision, weigh scale measurement system. The ADA4522-2 is used at the front end for amplification of the low level signal from the load cell.

Current flowing through a PCB trace produces an IR voltage drop; with longer traces, this voltage drop can be several millivolts or more, introducing a considerable error. A 1 inch long, 0.005 inch wide trace of 1 oz copper has a resistance of approximately 100 mΩ at room temperature. With a load current of 10 mA, the resistance can introduce a 1 mV error.

Therefore, a 6-wire load cell is used in the circuit. It has two sense pins, in addition to excitation, ground, and two output connections. The sense pins are connected to the high side (excitation pin) and low side (ground pin) of the Wheatstone bridge. The voltage across the bridge can then be accurately measured regardless of voltage drop due to wire resistance. The two sense pins are also connected to the ADC reference inputs for a ratiometric configuration that is immune to low frequency changes in the power supply excitation voltage.

The ADA4522-2 is configured as the first stage of a 3-op-amp instrumentation amplifier. It amplifies the low level amplitude signal from the load cell by a factor of $1 + 2R1/RG$. Capacitors C1 and C2 are placed in the feedback loops of the amplifiers and interact with R1 and R2 to perform low-pass filtering. This limits the amount of noise entering the Σ-Δ ADC. In addition, C3, C4, C5, R3, and R4 provide further common-mode and differential mode filtering to reduce noise and unwanted signals.

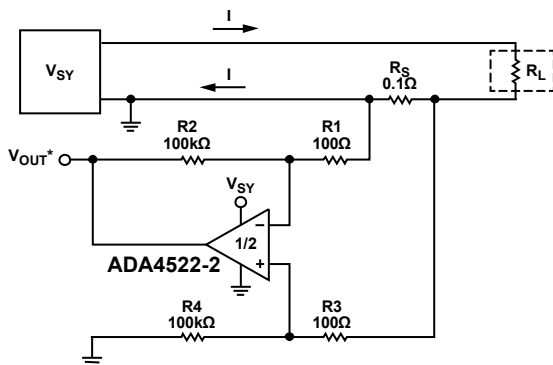


Figure 80. Precision Weigh Scale Measurement System

PRECISION LOW-SIDE CURRENT SHUNT SENSOR

Many applications require the sensing of signals near the positive or negative rails. Current shunt sensors are one such application and are mostly used for feedback control systems. They are also used in a variety of other applications, including power metering, battery fuel gauging, and feedback controls in industrial applications. In such applications, it is desirable to use a shunt with very low resistance to minimize series voltage drop. This not only minimizes wasted power, but also allows the measurement of high currents while saving power.

A typical shunt may be 100 mΩ. At a measured current of 1 A, the voltage produced from the shunt is 100 mV, and the amplifier error sources are not critical. However, at low measured current in the 1 mA range, the 100 μV generated across the shunt demands a very low offset voltage and drift amplifier to maintain absolute accuracy. The unique attributes of a zero drift amplifier provide a solution. Figure 81 shows a low-side current sensing circuit using the ADA4522-2. The ADA4522-2 is configured as a difference amplifier with a gain of 1000. Although the ADA4522-2 has high common-mode rejection, the CMR of the system is limited by the external resistors. Therefore, as mentioned in the Single-Supply Instrumentation Amplifier section, the key to high CMR for the system is resistors that are well matched from both the resistive ratio and relative drift, where $R1/R2 = R3/R4$.



* $V_{OUT} = \text{AMPLIFIER GAIN} \times \text{VOLTAGE ACROSS } R_S$
 $= 1000 \times R_S \times I$
 $= 100 \times I$

Figure 81. Low-Side Current Sensing

PRINTED CIRCUIT BOARD LAYOUT

The ADA4522-2 is a high precision device with ultralow offset voltage and noise. Therefore, take care in the design of the printed circuit board (PCB) layout to achieve optimum performance of the ADA4522-2 at the board level.

To avoid leakage currents, keep the surface of the board clean and free of moisture.

Properly bypassing the power supplies and keeping the supply traces short minimizes power supply disturbances caused by output current variation. Connect bypass capacitors as close as possible to the device supply pins. Stray capacitances are a concern at the outputs and the inputs of the amplifier. It is recommended that signal traces be kept at a distance of at least 5 mm from supply lines to minimize coupling.

A potential source of offset error is the Seebeck voltage on the circuit board. The Seebeck voltage occurs at the junction of two dissimilar metals and is a function of the temperature of the junction. The most common metallic junctions on a circuit board are solder to board traces and solder to component leads. Figure 82 shows a cross section of a surface-mount component soldered to a PCB. A variation in temperature across the board (where $T_{A1} \neq T_{A2}$) causes a mismatch in the Seebeck voltages at the solder joints, thereby resulting in thermal voltage errors that degrade the performance of the ultralow offset voltage of the ADA4522-2.

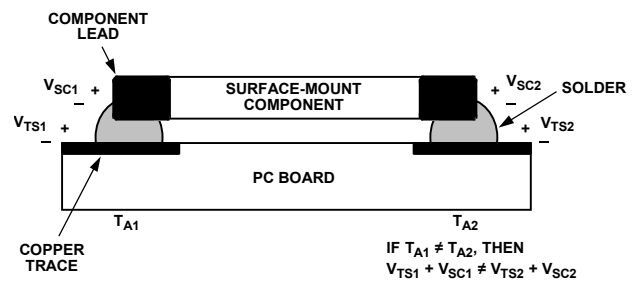


Figure 82. Mismatch in Seebeck Voltages Causes Seebeck Voltage Error

To minimize these thermocouple effects, orient resistors so that heat sources warm both ends equally. Where possible, it is recommended that the input signal paths contain matching numbers and types of components to match the number and type of thermocouple junctions. For example, dummy components, such as zero value resistors, can be used to match the thermoelectric error source (real resistors in the opposite input path). Place matching components in close proximity and orient them in the same manner to ensure equal Seebeck voltages, thus cancelling thermal errors. Additionally, use leads that are of equal length to keep thermal conduction in equilibrium. Keep heat sources on the PCB as far away from amplifier input circuitry as is practical.

It is highly recommended to use a ground plane. A ground plane helps distribute heat throughout the board, maintain a constant temperature across the board, and reduce EMI noise pick up.

COMPARATOR OPERATION

An op amps is designed to operate in a closed-loop configuration with feedback from its output to its inverting input. In contrast to op amps, comparators are designed to operate in an open-loop configuration and to drive logic circuits. Although op amps are different from comparators, occasionally an unused section of a dual op amp is used as a comparator to save board space and cost; however, this is not recommended for the ADA4522-2.

Figure 83 and Figure 84 show the ADA4522-2 configured as a comparator, with 10 kΩ resistors in series with the input pins. Any unused channels are configured as buffers with the input voltage kept at the midpoint of the power supplies. The ADA4522-2 has input devices that are protected from large differential input voltages by Diode D5 and D6, as shown in Figure 70. These diodes consist of substrate PNP bipolar transistors, and conduct whenever the differential input voltage exceeds approximately 600 mV; however, these diodes also allow a current path from the input to the lower supply rail, resulting in an increase in the total supply current of the system. Both comparator configurations yield the same result. At 30 V of power supply, I_{SY+} remains at 1.55 mA per dual amplifier, but I_{SY-} increases close to 2 mA in magnitude per dual amplifier.



Figure 83. Comparator Configuration A



Figure 84. Comparator Configuration B

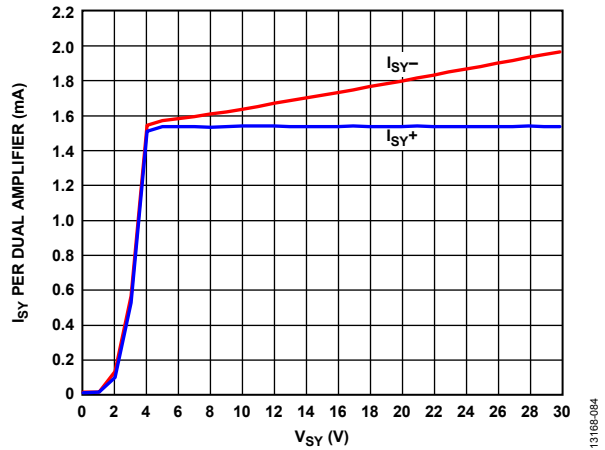


Figure 85. Supply Current (I_{SY}) per Dual Amplifier vs. Supply Voltage (V_{SY}) (ADA4522-2 as a Comparator)

Note that 10 kΩ resistors are used in series with the input of the op amp. If smaller resistor values are used, the supply current of the system increases much more. For more details on op amps as comparators, see AN-849 Application Note, Using Op Amps as Comparators.

OUTLINE DIMENSIONS

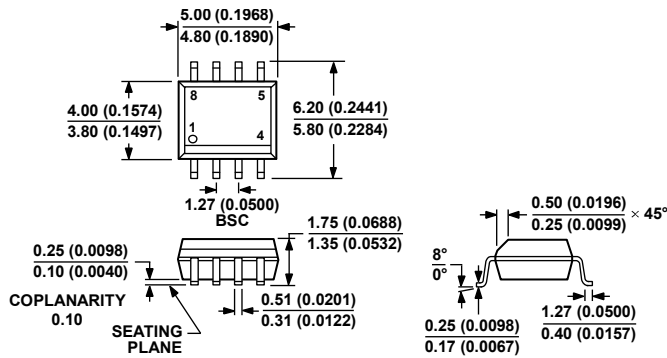


COMPLIANT TO JEDEC STANDARDS MO-187-AA

Figure 86. 8-Lead Mini Small Outline Package [MSOP] (RM-8)

Dimensions shown in millimeters

10-07-2009-B



COMPLIANT TO JEDEC STANDARDS MS-012-AA

CONTROLLING DIMENSIONS ARE IN MILLIMETERS; INCH DIMENSIONS (IN PARENTHESES) ARE ROUNDED-OFF MILLIMETER EQUIVALENTS FOR REFERENCE ONLY AND ARE NOT APPROPRIATE FOR USE IN DESIGN.

Figure 87. 8-Lead Small Outline Package [SOIC_N]

Narrow Body

(R-8)

Dimensions shown in millimeters

0124-07-A

ORDERING GUIDE

Model ¹	Temperature Range	Package Description	Package Option	Branding
ADA4522-2ARMZ	-40°C to +125°C	8-Lead Mini Small Outline Package [MSOP]	RM-8	A39
ADA4522-2ARMZ-R7	-40°C to +125°C	8-Lead Mini Small Outline Package [MSOP]	RM-8	A39
ADA4522-2ARMZ-RL	-40°C to +125°C	8-Lead Mini Small Outline Package [MSOP]	RM-8	A39
ADA4522-2ARZ	-40°C to +125°C	8-Lead Small Outline Package [SOIC_N]	R-8	
ADA4522-2ARZ-R7	-40°C to +125°C	8-Lead Small Outline Package [SOIC_N]	R-8	
ADA4522-2ARZ-RL	-40°C to +125°C	8-Lead Small Outline Package [SOIC_N]	R-8	

¹ Z = RoHS Compliant Part.

Данный компонент на территории Российской Федерации

Вы можете приобрести в компании MosChip.

Для оперативного оформления запроса Вам необходимо перейти по данной ссылке:

<http://moschip.ru/get-element>

Вы можете разместить у нас заказ для любого Вашего проекта, будь то серийное производство или разработка единичного прибора.

В нашем ассортименте представлены ведущие мировые производители активных и пассивных электронных компонентов.

Нашей специализацией является поставка электронной компонентной базы двойного назначения, продукции таких производителей как XILINX, Intel (ex.ALTERA), Vicor, Microchip, Texas Instruments, Analog Devices, Mini-Circuits, Amphenol, Glenair.

Сотрудничество с глобальными дистрибьюторами электронных компонентов, предоставляет возможность заказывать и получать с международных складов практически любой перечень компонентов в оптимальные для Вас сроки.

На всех этапах разработки и производства наши партнеры могут получить квалифицированную поддержку опытных инженеров.

Система менеджмента качества компании отвечает требованиям в соответствии с ГОСТ Р ИСО 9001, ГОСТ РВ 0015-002 и ЭС РД 009

Офис по работе с юридическими лицами:

105318, г.Москва, ул.Щербаковская д.3, офис 1107, 1118, ДЦ «Щербаковский»

Телефон: +7 495 668-12-70 (многоканальный)

Факс: +7 495 668-12-70 (доб.304)

E-mail: info@moschip.ru

Skype отдела продаж:

moschip.ru

moschip.ru_4

moschip.ru_6

moschip.ru_9